This manuscript was published as Huyst, A. M. R., Deleu, L. J., Luyckx, T., Meeren, L. V. D., Housmans, J. A. J., Grootaert, C., . . . Rousseau, F. (2022). Impact of heat and enzymatic treatment on ovalbumin amyloid-like fibril formation and enzyme-induced gelation. *FOOD HYDROCOLLOIDS*, *131*, 17 pages. doi:10.1016/j.foodhyd.2022.107784

Impact of heat and enzymatic treatment on ovalbumin amyloid-like fibril formation and enzyme-induced gelation

Arne M. R. Huyst[1], Lomme J. Deleu[2], Trui Luyckx[3], Louis Van der Meeren[4,5], Joëlle A. J. Housmans[6,7], Charlotte Grootaert[3], Margarita Monge-Morera[2], Jan A. Delcour[2], Andre G. Skirtach[4,5], Frederic Rousseau[6,7], Joost Schymkowitz[6,7], Koen Dewettinck[8] & Paul Van der Meeren[1]*

[1]Particle and Interfacial Technology Group (PaInT), Department of Green Chemistry and Technology, Faculty of Bioscience Engineering, Ghent University, Coupure Links 653, 9000 Ghent, Belgium

[2]Laboratory of Food Chemistry and Biochemistry and Leuven Food Science and Nutrition Research Centre (LFoRCe), Faculty of Bioscience Engineering, KU Leuven, Kasteelpark Arenberg 20, 3001 Leuven, Belgium

[3]Research Group Food Chemistry and Human Nutrition, Department of Food Technology, Safety and Health, Faculty of Bioscience Engineering, Ghent University, Coupure Links 653, 9000 Ghent, Belgium

[4]NanoBioTechnology laboratory, Department of Biotechnology, Faculty of Bioscience Engineering, Ghent University, Coupure Links 653, 9000 Ghent, Belgium

[5]Cancer Research Institute Ghent, 9000 Ghent, Belgium

[6]Switch Laboratory, VIB-KU Leuven Center for Brain & Disease Research, Herestraat 49, 3000 Leuven, Belgium

[7]Department of Cellular and Molecular Medicine, KU Leuven, Herestraat 49, box 802, 3000 Leuven, Belgium

[8]Food Structure & Function Research Group (FS&F), Department of Food technology, Safety and Health, Faculty of Bioscience Engineering, Ghent University, Coupure Links 653, 9000 Ghent, Belgium

Abstract

Heating aqueous solutions of ovalbumin (OVA) may cause gel formation. When heated at pH conditions close to the protein's isoelectric point (towards neutral pH), turbid particulate gels are formed, whereas at acidic pH fine-stranded, transparent gels are formed already at lower concentrations. Here, transparent gels were formed when subjecting 2.0% OVA to a combined heat (78 °C for 22 h at pH 7) and trypsin (37 °C for 48 h) treatment. Transmission electron microscopy clearly revealed the presence of long, straight OVA fibrils which contributed to the gel formation. Quartz crystal microbalance with dissipation (adsorption of small structures), size exclusion – HPLC (presence of both structures larger and smaller than native OVA) and atomic force microscopy (presence of long fibrils with a higher thickness, whereas heated OVA mainly showed amorphous aggregates) analyses confirmed that the additional enzymatic treatment was able to break down the amorphous aggregates formed by heating OVA into peptides, which then partly re-assembled into longer OVA fibrils. The above mentioned heat and enzymatic treatment conditions brought about gelation after 17 h with a gel strength of 68 Pa which broke at a stress of 38 Pa. By varying the temperature during heat (58-88 °C) and enzymatic (27-67 °C) treatments, gels were formed the fastest when heated at 78 °C followed by enzymatic treatment at 57 °C. A design of experiments for evaluating the impact of OVA and trypsin concentration revealed that the fastest gelation occurred at the higher considered OVA and trypsin concentrations. Additionally, the gel strength was also higher under the latter conditions. It is clear that different gel characteristics can be reached when varying the different process conditions, creating the opportunity for reconsidering the formulation of various foods such as jellies, marmalades and desserts.

Keywords: amyloid-like fibril; gelation; trypsin treatment; ovalbumin; design of experiments

Declarations of interest: none

*Corresponding author: Arne Huyst

Email: arne.huyst@ugent.be

Address: Particle and Interfacial Technology Group (PaInT), Department of Green Chemistry and Technology, Faculty of Bioscience Engineering, Ghent University, Coupure Links 653, Gent 9000, Belgium.

1. Introduction

Protein is one of the most essential macromolecules in human and animal dietary patterns. It not only accounts for a large part of our energy intake, it also fulfills many functional roles in our body (WHO, 2007). Protein gelation, emulsification and foaming properties have been studied extensively (Barbut, 1995; Lam & Nickerson, 2013; Mine, 2002; Poon, Clarke, & Schultz, 2001). Due to the ecological consequences of large scale animal (protein) production, food scientists study their partial or complete replacement by plant proteins or proteins with increased techno-functional properties (Asgar, Fazilah, Huda, Bhat, & Karim, 2010; Gumus, 2018; Stehfest et al., 2009). Within this framework, a type of ordered protein aggregates called amyloid-like fibrils (ALFs) has recently been studied in the context of food applications (Huyst et al., 2022, 2021; Jansens, Rombouts, et al., 2019; Lambrecht et al., 2021; Monge-Morera et al., 2020; Monge-Morera, Lambrecht, Deleu, Godefroidt, et al., 2021; Monge-Morera, Lambrecht, Deleu, Louros, et al., 2021).

Amyloid fibrils (AFs) were first studied regarding their function in certain human diseases (Chiti & Dobson, 2006; Nelson et al., 2005). Their presence was related to increased occurrence of Alzheimer, Parkinson and Diabetes type II (Harrison, Sharpe, Singh, & Fairlie, 2007). Later on, it was proven that many non-disease related proteins such as lysozyme (Krebs et al., 2000), whey protein isolate (WPI) (Loveday, Su, Rao, Anema, & Singh, 2011) and ovalbumin (OVA) (Pearce, Mackintosh, & Gerrard, 2007) also show fibrillation. X-ray diffraction analysis of AFs shows a distinct cross β-sheet pattern consisting of stacked β-strands (Sunde et al., 1997). The presence of these structures can be examined by thioflavin T (ThT) fluorescence, X-ray diffraction, circular dichroism or infrared spectroscopy and several microscopic techniques (Astbury, Dickinson, & Bailey, 1935; Khurana et al., 2005; Leonil et al., 1997; Rambaran & Serpell, 2008; Xue, Lin, Chang, & Guo, 2017). AF fibril formation was not studied by all of these methods in many earlier publications and it was argued in some publications that there are also fibrils that show limited ThT fluorescence (Lambrecht et al., 2021) or different X-ray diffraction patterns (Mackintosh et al., 2009). In these cases, the fibrillar structures are usually referred to as ALFs.

Fibril formation (*in vitro*) is mostly induced by increasing the temperature to start protein aggregation (Jansens, Rombouts, et al., 2019) or self-assembly (Abalymov et al., 2021). Fibril formation largely depends on temperature, pH and ionic strength conditions (Loveday, Anema, & Singh, 2017; Mezzenga & Fischer, 2013; Wei, Cheng, & Huang, 2019). It generally takes place at moderate heating (60-90 °C) at low pH (2-3) and low salt concentrations (0-1 M NaCl) (Swaminathan et al., 2011; Wang, Chen, & Hung, 2006). When heated at low pH, hydrolysis of β-lactoglobulin (β-lg) results in fibrillogenic and non-fibrillogenic peptides (Kroes-Nijboer, Venema, Bouman, & van der Linden, 2011). The former peptides were further considered to be the building blocks of ALFs (Gao, Xu, Ju, & Zhao, 2013).

However, most foods have a rather neutral pH, which makes highly acidic process conditions undesirable. ALF formation has also been studied at neutral pH for soy proteins (Mills, Huang, Noel, Gunning, & Morris, 2001), wheat gluten proteins (Lambrecht et al., 2021), OVA (Pearce et al., 2007; Tanaka et al., 2011) and even whole hen egg white (HEW) (Monge-Morera et al., 2020). However, ALFs formed at neutral pH conditions are much shorter than those at lower pH (Loveday et al., 2011) and present in smaller quantity (Jansens, Rombouts, et al., 2019). Amorphous aggregates have also been retrieved (Lambrecht et al., 2019). Therefore, the ALFs formed at neutral pH might be less functional.

One of the considered techniques to overcome this problem and stimulate ALF formation at neutral pH is enzymatic treatment with trypsin (Lambrecht et al., 2019). This proteolytic enzyme is mainly secreted by the pancreas as trypsinogen. In the small intestine it can cleave protein structures after

lysine and arginine residues (Simpson, 2006). As these amino acid residues are not likely to be present in fibrillation prone regions (Monge-Morera, Lambrecht, Deleu, Louros, et al., 2021), trypsin cleavage does not negatively impact subsequent fibrillation or the fibrils present. Knauer, Soreghan, Burdick, Kosmoski, & Glabe (1992) indeed observed that Alzheimer Aβ42-43 AFs resist this type of proteolysis. However, trypsin can hydrolyze the α-helix and β-sheet structure in proteins and transform amorphous aggregates (mainly formed upon heating at rather neutral pH) into peptides. Enzymatic treatment can thus be used to break down amorphous aggregates into peptides, which can form long, mature ALFs, finally resulting in a mixture of ALFs and non-fibrillogenic peptides (Lambrecht et al., 2019). Monge-Morera et al. (2020) found that tryptic incubation of heated OVA (78 °C for 22 h) or HEW (100 °C for 15 min) results in the formation of both (long) curly and straight fibrils. In contrast, other authors claimed that fibrils are broken down by trypsin treatment (Emeson & Kikkawa, 1959; Holm et al., 2007). Emeson & Kikkawa (1959) found that tryptic digestion at pH 8 for 48 h of AFs from the liver of tuberculosis patients resulted in a shift from dense fibrillar bundles (100 Å) to thinner bundles (40 Å). Nevertheless, the morphology was not affected, and the impact of the enzymatic treatment thus seemed rather low. However, Holm et al. (2007) did show a significant degradation of bovine serum albumin fibrils into shorter fragments as a result of tryptic treatment at pH 7.4.

ALFs have been considered to improve the gel properties (Bolder, Hendrickx, Sagis, & van der Linden, 2006; Nicolai & Durand, 2013; Weijers, Sagis, Veerman, Sperber, & van der Linden, 2002). Gels can stabilize dispersions, foams and emulsions (Martin, Grolle, Bos, Cohen Stuart, & van Vliet, 2002; Murray, 2011). They can also be considered as compounds for controlling the release of aroma compounds (Humblet-Hua, Scheltens, van der Linden, & Sagis, 2011) or as thickening agents (Akkermans, van der Goot, Venema, van der Linden, & Boom, 2008; Mudgal, Daubert, & Foegeding, 2009). Gel structures are present in several foods such as yoghurt, dressing, marmalade, candy and some desserts (Banerjee & Bhattacharya, 2012). Gelation of ALF dispersions has mainly been observed as a result of heating under acidic conditions (Loveday, Wang, Rao, Anema, & Singh, 2012; Weijers et al., 2002). However, extended heating of β-lg results in shorter fibrils and is accompanied with a tenfold reduced viscosity (Loveday, Wang, et al., 2012). For this reason, it is believed that the reduced fibril length to thickness ratio (i.e. its aspect ratio) impacts its stiffness and thus its gelling capacity (Loveday, Su, Rao, Anema, & Singh, 2012). The latter was ascribed to entanglement of the long fibrils which results in a fine-stranded network. Gels obtained from dispersions containing ALFs are transparent when formed by heating at a pH further away from the isoelectric point (pI) in the presence of low concentrations of salt (Nicolai & Durand, 2013; van der Linden & Venema, 2007). Under such conditions, the electrostatic forces are repulsive and the fine protein fibrils form a network which hardly scatters light. In contrast, heating close to pI or in the presence of high salt concentrations results in particulate gelation and turbid gels consisting of randomly aggregated protein structures which scatter light (Ako, Nicolai, & Durand, 2010; Ako, Nicolai, Durand, & Brotons, 2009). A well-known example of a particulate gel is that obtained when boiling HEW due to the different pIs of the proteins present (Zayas, 1997).

Particulate gels are subject to syneresis (Ikeda & Li-Chan, 2004) and have a limited gel strength (Van Kleef, 1986) and hardness (Hatta, Kitabatake, & Doi, 1986). In contrast, fine-stranded gels do not only form stronger gels, but also have an improved water-binding capacity (Barbut, 1995; Hongsprabhas & Barbut, 1996). At similar protein concentrations, heating proteins at neutral pH results in weaker gels than heating under acidic conditions (Renkema, Lakemond, de Jongh, Gruppen, & van Vliet, 2000). The previously mentioned short fibril length when proteins are heated at neutral pH limits the extent of

fibrillar entanglements which induces gelation. The present work covers ALF formation from OVA, being the primary [54.0% (w/w)] protein in HEW, upon heating at neutral pH and subsequent enzymatic treatment. As such, the hypothesis by Lambrecht et al. (2019) that enzymatic treatment resulted in long, mature ALFs was evaluated. Furthermore, it was experimentally verified whether the heated and trypsin treated OVA dispersions can form viscous, gel-like structures. The influence of the temperature during heating and enzymatic treatment, as well as the impact of protein and trypsin concentration thereupon were evaluated. As such, process conditions were found for swiftly forming strong gels which can be considered for stabilizing oil-in-water (O/W) emulsions.

2. Materials and methods

2.1. Materials

OVA (albumin from chicken egg-white, 90% pure protein) was obtained from Sigma-Aldrich (Merck, Overijse, Belgium). Trypsin from porcine pancreas [EC 3.4.21.4.; 13,000 – 20,000 N-benzoyl-L-arginine ethyl ester units/mg protein], ThT, sodium azide, 8-anilino-1-naphthalenesulfonic acid (ANS), concentrated sulfuric acid, 32% NaOH, boric acid, titrisol HCl, 25% ammonia, 30% hydrogen peroxide and 1-hexadecanethiol were also purchased from Sigma-Aldrich. Disodium hydrogen phosphate and sodium dihydrogen phosphate were acquired from Acros Organics (Geel, Belgium). Hellmanex III, 99% ethanol, 3.0% (w/v) uranyl acetate and Kjeltab CX were bought from VWR (Leuven, Belgium).

2.2. Preparation and pretreatment of ovalbumin dispersions

OVA [2.0% (w/v)] was dissolved in demineralized water (pH 6.6) containing 0.02% (w/v) sodium azide to prevent microbial spoilage. These samples were stored overnight and are referred to as unheated (UH) OVA dispersions. Part of the dispersions was heated in 40 mL EPA screw neck borosilicate glass vials (EP Scientific, Waltham, MA, USA) in a water bath at 78.0 °C for 22 h as described by Alting et al. (2004). Afterwards, they were rapidly cooled and are further referred to as heated (H) OVA dispersions. After adding 200 µL 2.0% (w/v) trypsin (ca. 0.26-0.40 enzyme units/µL) to 25.0 mL H OVA dispersion (i.e. 8 µL trypsin solution for each mL H OVA dispersion), they were further incubated for 48 h at 37.0 °C to allow enzymatic digestion. The samples were cooled to room temperature and are further referred to as heated and trypsin treated (H TT) OVA dispersions. A similar UH OVA dispersion was subjected to this enzymatic treatment and is further referred to as UH TT OVA. As enzyme-free references, UH and H OVA dispersions were also subjected to the prior incubation treatment without adding trypsin. The resultant samples after cooling to room temperature are referred to as UHinc and Hinc, respectively. All samples were stored at 5 °C until further analysis.

2.3. Preparation of enzymatically treated ovalbumin gels

Further evaluation of the H TT OVA gelation was done by varying both preheating (58 °C – 68 °C – 78 °C – 88 °C) and trypsin-incubation (27 °C – 37 °C – 47 °C – 57 °C – 67 °C) temperatures. During these experiments, the OVA concentration (2.0%), trypsin quantity (8 µl of 2.0% trypsin solution per mL OVA dispersion), preheating time (22 h) and incubation time (48 h) were kept constant. Based on the outcome of these experiments, preheating and incubation temperatures of 78 °C and 57 °C, respectively, were considered to be optimal and were chosen for the further experiments.

Next, an experimental (response surface) design using the I-optimal criterion was used to identify the OVA concentration and quantity of 2.0% trypsin which led to the fastest gelation and highest gel strength (see section 2.14). The design of experiments (DOE) considered both factor main effects, as well as interaction and quadratic effects (Goos & Jones, 2011). To this end, the OVA concentration was

varied between 2.0, 3.0 and 4.0%, whereas the trypsin quantity varied between 8, 16 and 24 µL trypsin, respectively, for each mL H OVA dispersion. In total, 9 different factor levels were combined with 1 repetition each, except for the central point (3.0% OVA and 16 µL trypsin solution per mL H OVA dispersion) which had 4 replicates (Table 2). To simplify the interpretation of the surface designs, the factors were normalized from -1 over 0 to +1, corresponding with the lowest, middle, and highest factor value, respectively.

2.4. Characterization of fibril formation in ovalbumin dispersions

2.4.1. Microscopy imaging

Transmission electron microscopy imaging was done as previously described (Huyst et al., 2021). For atomic force microscopy, the H and H TT OVA samples were diluted to a protein concentration of 0.1% (w/v) using demineralized water. Aliquots (10 µL) were added to freshly cleaved mica (Agar Scientific, Stansted, UK) and were subsequently washed five times with milliQ water. Finally, the mica was dried using nitrogen gas. Images were acquired using a NanoWizard 4 (Bio-atomic force microscope, JPK/Bruker, Berlin, Germany) with a ppp-NchAu cantilever (Nanosensors, Neuchatel, Switzerland) in the tapping mode. Further image processing was performed using Fiji software (ImageJ) to calculate the average length distribution of 30 randomly selected ALFs in each sample.

2.4.2. Analysis of fluorescence

ThT fluorescence measurements were performed according to the method described by Huyst et al. (2021). In addition, the surface hydrophobicity of the different dispersions was determined by measuring the ANS fluorescence as described by Lambrecht, Rombouts, De Ketelaere, & Delcour (2017). The estimated concentrations (0.05-0.5 mg/mL) were then related to the real concentrations of the original dispersions, as determined by Kjeldahl analysis (N x 6.25). Finally, a linear regression curve was fitted to the data of each dispersion. As such, the obtained slope was considered as a measure to compare the surface hydrophobicity, expressed as arbitrary units (AU) per mg/mL.

2.4.3. Analysis of secondary protein structure

Analysis of the secondary protein structures of the different OVA samples was done using circular dichroism (CD) as described by Huyst et al. (2021). Dichroweb software (Lobley, Whitmore, & Wallace, 2002; Whitmore & Wallace, 2004) was used to deconvolute the different CD spectra using the SELCON3 deconvolution algorithm (Sreerama & Woody, 2000) into the relative contributions of α-helix, β-strand, β-turn and unordered structures.

2.4.4. Analysis of size exclusion-high performance liquid chromatography

For size exclusion-high performance liquid chromatography (SE-HPLC) analysis, the samples were treated essentially as mentioned by Huyst et al. (2021).

2.5. Detection of peptides in ovalbumin dispersions

Quartz crystal microbalance with dissipation (QCM-D) analysis was performed on 0.1% UH, H and H TT OVA dilutions according to the method described by Setiowati, De Neve, A'yun, & Van der Meeren (2021).

2.6. Characterization of gelling properties of ovalbumin gels

2.6.1. Analysis of viscosity

The viscosity (µ) of the different dispersions was measured using a Brookfield (Kruibeke, Belgium) LV-DVII+ pro viscometer equipped with a small sample adapter. All measurements were performed at

20.0 °C and at rotational speeds increasing from 10 to 200 rpm. When the SC4-18 (low viscosity samples) spindle was used (UH, H, Hinc, UHinc and UH TT OVA), this corresponded with a shear rate ($\dot{\gamma}$) range from 13.2 to 264.0 s^{-1}, whereas for the SC4-34 (higher viscosity samples) spindle (H TT OVA), this corresponded to shear rates ranging between 2.8 and 56.0 s^{-1}. Each speed was maintained for 30 s and five datapoints were collected at each rotational speed. Afterwards, the data points having a torque lower than 10% were removed, the remaining data were averaged at each speed, plotted in function of the corresponding shear rate, and a power law equation was fitted:

$$\mu = C * \dot{\gamma}^{(n-1)}$$

with C the consistency coefficient (mPa.s) and n the flow behavior index.

As such, the C values were used to compare samples measured with different spindles. It is of note that when no power law could be fitted (which was the case for low-viscous samples with Newtonian behavior), the consistency coefficient was determined by calculating the average viscosity over all shear rates.

2.6.2. Small amplitude oscillatory shear rheology

Oscillatory shear measurements were performed on the H TT OVA dispersions with an AR 2000ex rheometer (TA instruments, Antwerp, Belgium) equipped with a concentric cylinder DIN geometry. Aliquots [8-24 µL (ca. 0.26-0.40 enzyme units/µL)] of 2.0% trypsin solution per mL H OVA dispersion were added to 2.0-4.0% H OVA dispersions which had been preheated at 58-88 °C for 22 h. These mixtures were then incubated at 27-67 °C for 12-48 h in the rheometer (time sweep). A constant frequency and strain of 1 Hz and 0.01%, respectively, were considered. The measurements of both the elastic (G') and viscous (G") moduli occurred each 30 s. Before the time sweep, a conditioning time of 5 min was employed for equilibrating the sample temperature. A solvent trap on top of the concentric cylinder prevented excessive evaporation. Afterwards, a frequency sweep was performed to assess the gel strength. The frequency was increased from 0.01 Hz to 10.0 Hz at a constant oscillating stress of 0.5 Pa. Finally, a stress sweep (amplitude sweep) was executed to validate whether the previous conditions were within the linear viscoelastic region. Here, the stress was increased from 0.1 to 1000.0 Pa at a constant frequency of 1 Hz.

The gelation time was defined as the cross-over time at which G' and G" intersect and G' becomes larger at longer time. Furthermore, G'_{LVR}, an indication of the gel strength in the linear viscoelastic region (LVR) was calculated as the average of only the G' values of the amplitude sweep that remained constant. Furthermore, σ* was defined as the shear stress at which G' became smaller than 90% of the G'_{LVR}, G* is the square root of the sum of the squared values of G' and G" within the LVR and tan(ϕ) (i.e. a measure of the gel brittleness) is the ratio of G" over G' in the LVR.

2.6.3. Low resolution nuclear magnetic resonance

Nuclear magnetic resonance (NMR) experiments were conducted using a temperature-regulated (set at 5 °C) Spin Track NMR spectrometer (Resonance systems, Kirchheim, Germany) with the accompanying Relax8 software. The enzymatic treatments (gelation step) at the different conditions considered in the DOE (Table 2) were performed in the NMR tubes filled to a height of 18 mm. The samples were submitted to a Carr Purcell Meiboom Gill (CPMG) experiment with a characteristic frequency of 22.61 MHz. The latter was performed with a 90° RF pulse of 2.5 µs and a pulse train of 180° at a pulse length of 5.8 µs. Optimized echo sequences were performed based on the anticipated

T_2 values of 500, 300 and 250 ms for 2.0, 3.0 and 4.0% OVA samples, respectively. The acquired CPMG data were fitted using MATLAB software to an exponential decaying function as a function of time (t):

$$I(t) = I_0 * e^{-R_2 * t}$$

With I_0 the initial intensity and R_2 the relaxation rate which equals $1/T_2$ (spin-spin relaxation time).

2.7. Statistical analysis

A single factor ANOVA test (one-way ANOVA) with R software was performed to compare samples. This was combined with post-hoc analysis using the Tukey procedure to perform pairwise comparisons. Differences of triplicates were considered to be significant at $p < 0.05$. In contrast, the different slopes of linear regression curves of the ANS fluorescence data were compared by analysis of covariance (ANCOVA).

The different parameters derived from rheological measurements (section 2.12) were used to fit the response surface model (see section 2.3) using the least sum of squares regression for identifying significant effects ($p < 0.1$). The full model was fitted, and backward model selection was considered to remove insignificant effects.

3. Results and discussion

3.1. Characterization of ovalbumin dispersions

3.1.1. Atomic force microscopy and transmission electron microscopy visualization

We first evaluated whether enzymatic treatment resulted in long, mature ALFs and used atomic force microscopy (AFM) and TEM to study both H and H TT OVA samples.

In case of H OVA, AFM images (Figure 1A) showed mainly randomly shaped (amorphous aggregates and/or native protein) and some short, worm-like (ALFs) structures. In contrast, H TT OVA dispersions contained much more fibrils, with a broader length distribution (Figure 1B). Furthermore, amorphous aggregates could not be detected in the latter sample.

The length distribution of ALFs in both samples was compared by length calculation of 30 randomly picked fibrillar structures using Fiji (ImageJ) software (Figure 1C-D). The lengths of the worm-like structures present in H OVA were mainly between 100 and 150 nm. In contrast, the largest fraction of ALFs present in H TT OVA had lengths between 650 and 825 nm. This clearly indicated that the enzymatic treatment indeed resulted in longer, flexible ALFs. Therefore, the suggestion by Lambrecht et al. (2019) that fibril formation can be enhanced at the expense of amorphous aggregates, was confirmed.

Next to the difference in fibrillar length, also their height was clearly different. Whereas H OVA ALFs showed a maximum height of 0.53 nm, this was fivefold larger for H TT OVA (2.81 nm). The latter samples clearly showed that a maximum was reached at dense spots, which was probably related to accumulation of multiple ALFs. Nevertheless, even the single fibrils had a height of about 1 to 2 nm which was still higher than for H OVA. These observations provide support for the view that enzymatic digestion facilitates the formation of mature fibrils due to entanglement of multiple protofibrils, thus increasing their thickness.

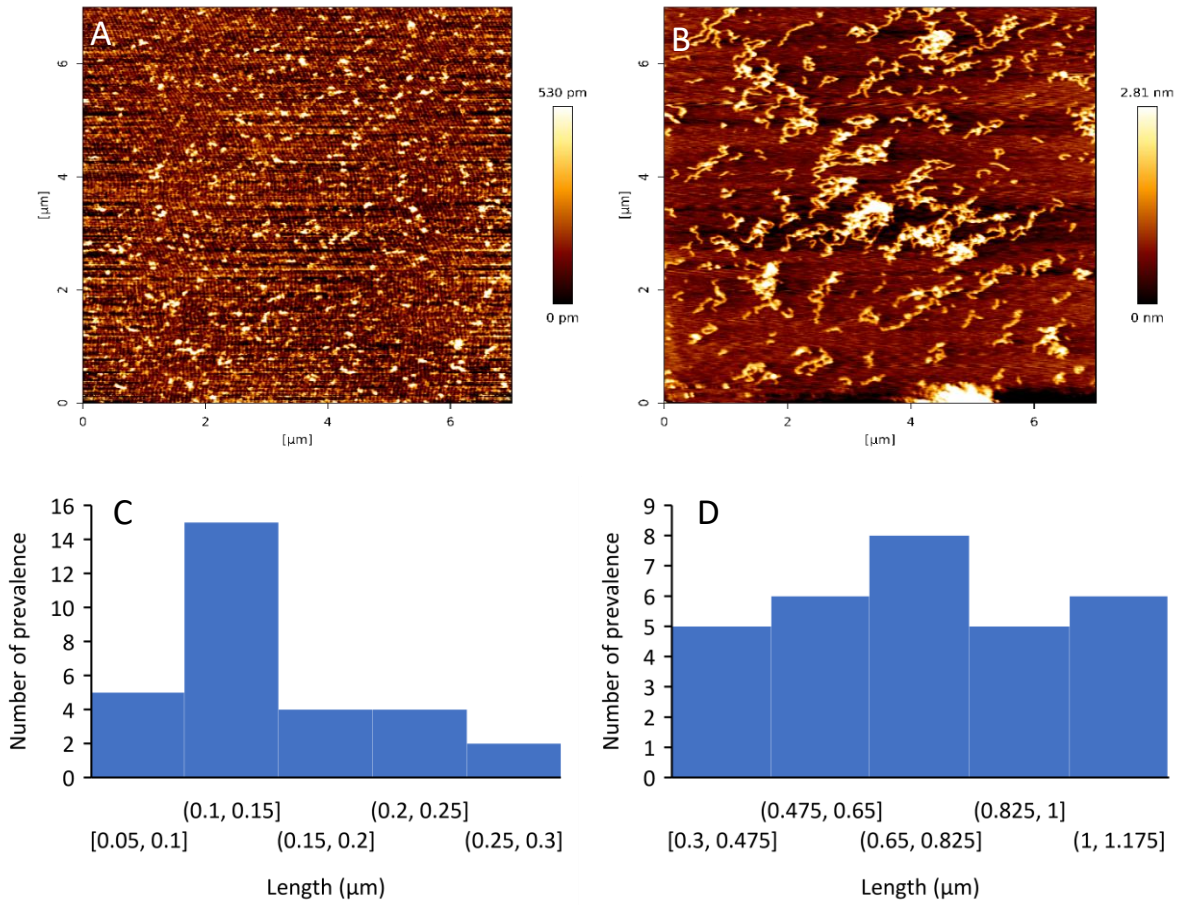

Figure 1: Atomic force microscopy (AFM) images of dispersions from ovalbumin heated for 22 h at 78 °C (H OVA, A) and subsequently incubated with trypsin at 37 °C for 48 h (H TT OVA, B). Length distribution of fibrillar structures based on 30 randomly selected structures of H OVA (C) or H TT OVA (D) dispersions.

Both H OVA and H TT OVA dispersions were also visualized by TEM (Figures 2 and S1). H OVA dispersions clearly contained a mixture of random aggregates and some small, worm-like structures. In contrast, H TT OVA dispersions showed much longer ALFs which were intertwined to some extent. Furthermore, the latter samples also contained both straight and curly fibrils. The presence of straight fibrils has already been described by Monge-Morera et al. (2020) for similarly treated OVA samples.

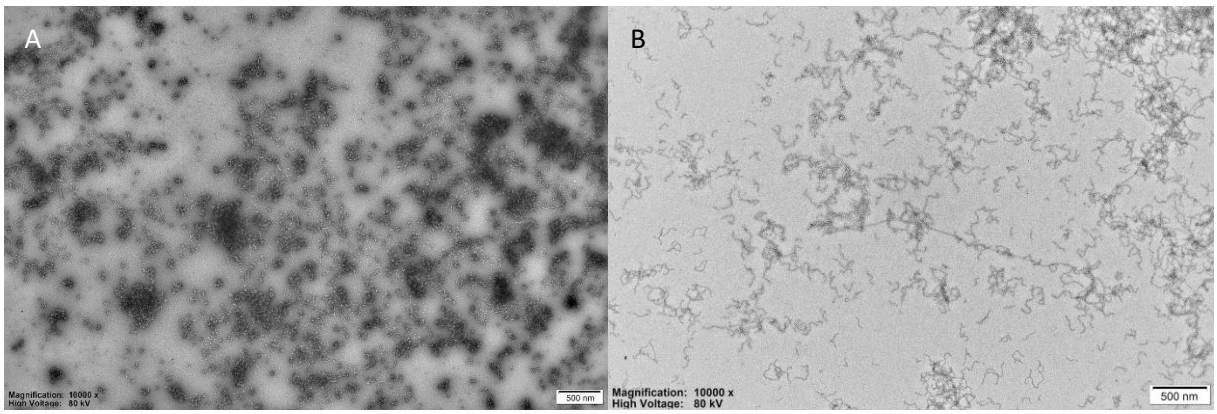

Figure 2: Transmission electron microscopy (TEM) images of negatively stained dispersions from ovalbumin heated for 22 h at 78 °C (H OVA, A) and subsequently incubated with trypsin at 37 °C for 48 h (H TT OVA, B). Both images were taken with a 10000x magnification, and the length scales correspond to a distance of 500 nm.

3.1.2. Relative thioflavin T fluorescence

Relative ThT fluorescence was assessed to validate possible effects of heat and enzymatic treatment on ALF formation (Figure 3, blue). Although UH OVA dispersions were thought to contain no ALFs, their relative ThT fluorescence [4.40 ± 0.87 %/(g/L)] revealed that low quantities of ALFs may have been present. Similar observations were made before for HEW by Monge-Morera et al. (2020). In contrast, the relative ThT fluorescence for H OVA dispersions was determined as 47.00 ± 0.74 %/(g/L), in line with previous observations (Monge-Morera et al., 2020; Pearce et al., 2007), and showing the formation of ALFs upon heating ($p = 0.00$). As claimed before by Lambrecht et al. (2019), heating native protein structures results in partial denaturation, which in its turn may lead to formation of both amorphous and short fibrillar aggregates.

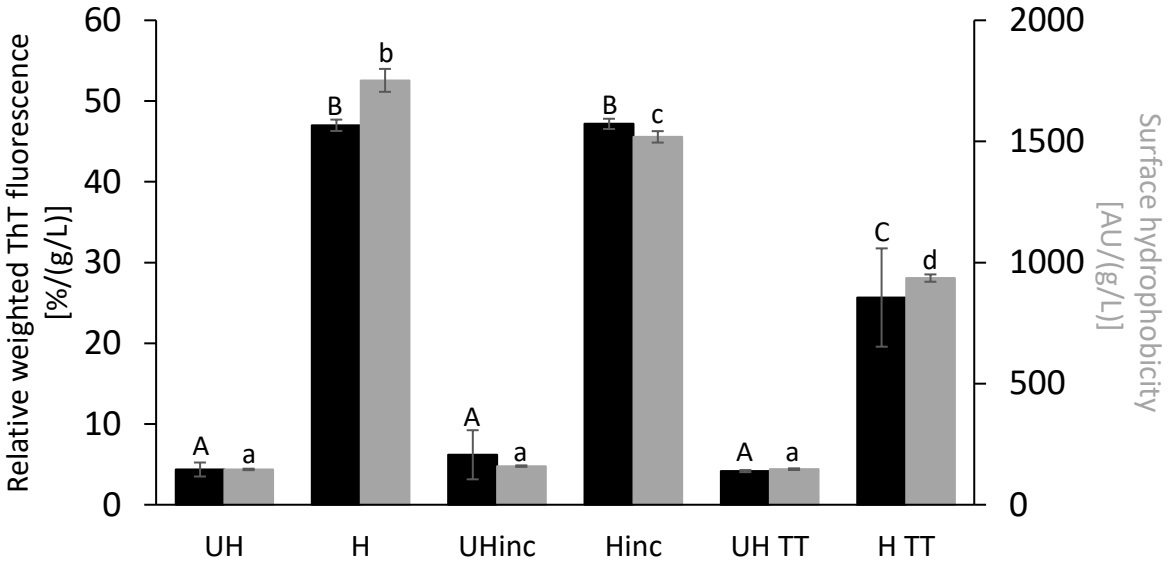

Figure 3: Relative weighted Thioflavin T (ThT) fluorescence (black) and surface hydrophobicity as determined by 8-anilino-1-naphthalenesulfonic acid (ANS) fluorescence (grey) of the different (pretreated) OVA samples which are labelled as discussed in section 2.2. Significant differences between relative ThT fluorescence (capital letters) and between surface hydrophobicity (small letters) values were determined at the 95% confidence interval ($p < 0.05$): significant differences are indicated by different letters.

H OVA dispersions were further incubated with trypsin during 48 h at 37 °C to enable tryptic digestion. The latter treatment caused the relative ThT fluorescence of H TT OVA dispersions to decrease to 25.66 ± 6.09 %/(g/L). This was in accordance with the observation of Holm et al. (2007) who reported a decreased ThT fluorescence upon incubation of heated bovine serum albumin with trypsin. The latter authors suggested that fibrils were broken down to structures that showed less ThT fluorescence. However, their study did not include microscopy images which could have proven the breakdown of fibrillar structures. In contrast, the microscopic images discussed in section 3.1.1 clearly showed long fibrils after the enzymatic treatment. This confirmed the work of Monge-Morera et al. (2020) in which a similar reduction in relative ThT fluorescence upon an additional trypsin treatment on H OVA was found and associated to the presence of larger fibrils. Lambrecht et al. (2019) suggested that such additional trypsin incubation after heating leads to the formation of nicked protein structures from amorphous aggregates, and eventually peptides that either are fibrillogenic or non-fibrillogenic. The first type was suggested to build larger fibrillar structures upon incubation, whereas the latter peptides remained present in solution. According to Lambrecht, Schymkowitz, et al. (2019), fibrillar structures

remain largely unaffected, suggesting that cross β-sheet structures are not degraded during enzymatic treatment. Therefore, the lower relative ThT fluorescence of H TT OVA than of H OVA was suggested to rather be due to a more limited access between ThT and the longer fibrils.

Similar trypsin treatment on UH OVA showed that no fibrillation occurred under these conditions. Therefore, it is suggested that the extent of ALF formation observed for H TT OVA is mainly due to prior breakdown of amorphous aggregates into peptides. Kato, Watanabe, Nakamura, & Sato (1983) observed that trypsin cannot cleave UH OVA into sufficiently small peptides. Indeed, whereas UH OVA which had been subjected to tryptic digestion (24 h at 38 °C) was not hydrolyzed, a similar treatment on OVA which had been heated at 80 °C resulted in significant hydrolysis. Trypsin mainly acts on the positively charged residues lysine and arginine of which there are 20 and 15 in OVA, respectively (Nisbet, Saundry, Moir, Fothergill, & Fothergill, 1981). Both amino acids can act as gatekeepers next to aggregation prone regions to prevent aggregation (Rousseau, Serrano, & Schymkowitz, 2006). In native form, some of them are buried within the hydrophobic core (Israelachvili, 2011), lowering the number of accessible cleavage sites. In contrast, hydrophobic groups are more exposed when subjected to prior heating, making them prone to enzymatic hydrolysis and thus enabling the aggregation prone regions to induce aggregation (fibrillation).

Finally, the relative ThT fluorescence of UHinc OVA and Hinc OVA samples which only had been subjected to the 48 h incubation at 37 °C (without trypsin) suggested that the latter treatment alone did not influence ALF formation, as the fluorescence was not significantly different from that of both UH OVA ($p = 0.81$) and H OVA ($p = 0.96$) samples.

3.1.3.8-Anilino-1-naphthalenesulfonic acid fluorescence

ALF formation not only leads to an increase in ThT fluorescence, it is also accompanied by changes in surface hydrophobicity (Figure 3, grey). Whereas native OVA (UH OVA) has a globular structure shielding its hydrophobic groups, heating OVA (H OVA) implies unfolding of the globular structure which significantly increases its surface hydrophobicity ($p = 0.00$). The present findings are in line with observations of Mohammadian et al. (2019) and Zhao et al. (2018) for WPI and β-lg, respectively.

Furthermore, tryptic hydrolysis is expected to release peptides with increased surface hydrophobicity as the cleavage occurs next to hydrophobic amino acids (Gao et al., 2013). However, both UH TT and H TT samples had a significantly ($p = 0.00$) lower surface hydrophobicity than H OVA. For UH TT OVA, this logically followed from the limited hydrolysis taking place in the native protein, as discussed above (not significantly different from UH OVA; $p = 1.00$). For H TT OVA, this was in line with the results of ThT fluorescence and microscopic evidence which indicated the presence of mature fibrils. Fibril formation is suggested to occur through self-assembly of monomeric proteins, being either native proteins (at neutral pH) or peptides (following acidic or enzymatic digestion) (Arnaudov, de Vries, Ippel, & van Mierlo, 2003). The monomers first form oligomers, which further assemble into protofibrils and eventually entangle into mature fibrils. Meratan, Ghasemi, & Nemat-Gorgani (2011) observed that ANS fluorescence of HEW lysozyme increased during a heat treatment (57 °C, 6 days, pH 2.2) in which mainly oligomers and protofibrils were formed, whereas longer incubation resulted in mature fibrils with a significantly reduced surface hydrophobicity. Gao et al. (2013) observed that whey protein concentrate (WPC) also resulted in an increased ThT fluorescence when heated at 90 °C for up to 10 h, whereas the corresponding surface hydrophobicity [initial 495.6 ± 7.7 AU] increased to a maximum

after 6 h [1217 ± 34 AU], before declining again after 10 h [900 ± 29.1 AU]. Hence, these results indicate that very large mature ALFs interact to a lesser extent with ANS. Similar observations were made by Alavi, Chen, & Emam-Djomeh (2021). Indeed, adding sodium hexametaphosphate to HEW resulted in larger fibrillar structures with a reduced surface hydrophobicity. The authors claimed this to be due to the presence of large structures which made it more difficult for ANS to reach the hydrophobic patches.

The increased relative ThT fluorescence results observed here indicate that heating OVA at neutral pH induced ALFs. However, they could not be considered as mature fibrils. In contrast, the lower relative ThT fluorescence of H TT OVA dispersions, as discussed in section 3.1.2, is suggested to be due to the presence of large mature fibrils which limit the extent of both ANS-ALF and ThT-ALF interactions. In accordance with the observations by Gao et al. (2013) for long WPC fibrils, the sample with longer fibrils (H TT OVA) had a higher surface hydrophobicity than the native protein (UH OVA).

Lastly, UH OVA and UHinc OVA showed similar surface hydrophobicity indicating that the incubation for two days at 37 °C did not have an impact thereupon. In contrast, the surface hydrophobicity of Hinc OVA was slightly lower than that of H OVA. However, this effect was negligible in comparison to the decrease when comparing with the H TT OVA sample.

3.1.4. Circular dichroism

The secondary structure of the protein in the different dispersions can provide additional information about ALF formation. CD was here performed to study the relative contribution of β-sheet structures (Figure 4A). Evidently, all spectra of OVA dispersions which had not been heated (UH, UHinc and UH TT OVA) were similar, showing a broad valley with minima around 212 and 225 nm. These distinct minima are closely related to samples rich in α-helix (Kelly, Jess, & Price, 2005). That mainly α-helix structures were detected confirmed that little if any ALFs were present, as also deduced from the relative ThT fluorescence results (section 3.1.2).

In contrast, the different heated samples (H, Hinc and H TT OVA) showed distinct profiles with a single valley. Both H and Hinc samples showed a minimum near 215 nm, corresponding with the presence of anti-parallel β-sheets (Kelly et al., 2005), which further suggested that both samples contained an increased contribution of β-sheets, in line with the relative ThT fluorescence data. Similar shifts were observed when heating WPC for 10 h at 90 °C (Gao et al., 2013). Lastly, the CD pattern of the H TT OVA dispersions had a minimum at lower wavelength (at about 205 nm) than those of H and Hinc OVA. This indicated that they contained less α-helix and more unordered non-fibrillogenic peptide structures along with ALFs (β-sheets). Indeed, next to the characteristic profile of α-helix and β-sheets, Kelly et al. (2005) also depicted the profile of unordered, irregular structures. The latter had a single valley with a minimum around 195 nm. Lara, Gourdin-Bertin, Adamcik, Bolisetty, & Mezzenga (2012) observed a similar shift for filtrates (100 kDa molecular weight cut-off) containing residual peptides after acidic hydrolysis when heating OVA dispersions for 170 h at 90 °C at pH 2.

Further elucidation of the contribution of the different secondary structures was performed using a SELCON3 algorithm. The profiles of UH OVA (0 h), H OVA (0.5 to 22 h) and subsequently enzymatically treated H TT OVA (22.5 to 60 h) dispersions were deconvoluted into their α-helix, β-sheet, β-turn and unordered structure contents. It is clear from Figure 4B that UH OVA consisted mainly of α-helix (77.3%) and to a lesser extent of β-sheets (1.2%), β-turns and unordered structures (21.5%). The latter

observations were in line with the low relative ThT fluorescence of UH OVA. Upon heating, the α-helix content decreased to 43.6% (22 h at 78 °C), whereas the β-sheet (12.0%) and combined β-turn and unordered structures (44.4%) content increased. The enrichment of β-sheet structures suggested the formation of ALFs (Arnaudov & de Vries, 2005). Regretfully, no information could be gained regarding their length. Subsequent trypsin treatment showed a further reduction of the α-helix content (to 33.6%). However, the contribution of β-sheets (11.6%) remained constant and mainly additional β-turns and unordered structures (54.8%) were formed. The constant level of β-sheets suggests that no additional fibrils were formed upon enzymatic treatment, but that they were longer than those in the H OVA dispersions. Whereas the additionally formed unordered structures may be assigned to non-fibrillogenic peptides, the increase in β-turns could not be explained. However, the similar CD patterns of either β-turns or unordered structures (Kelly et al., 2005) makes it difficult to distinguish between the two fractions.

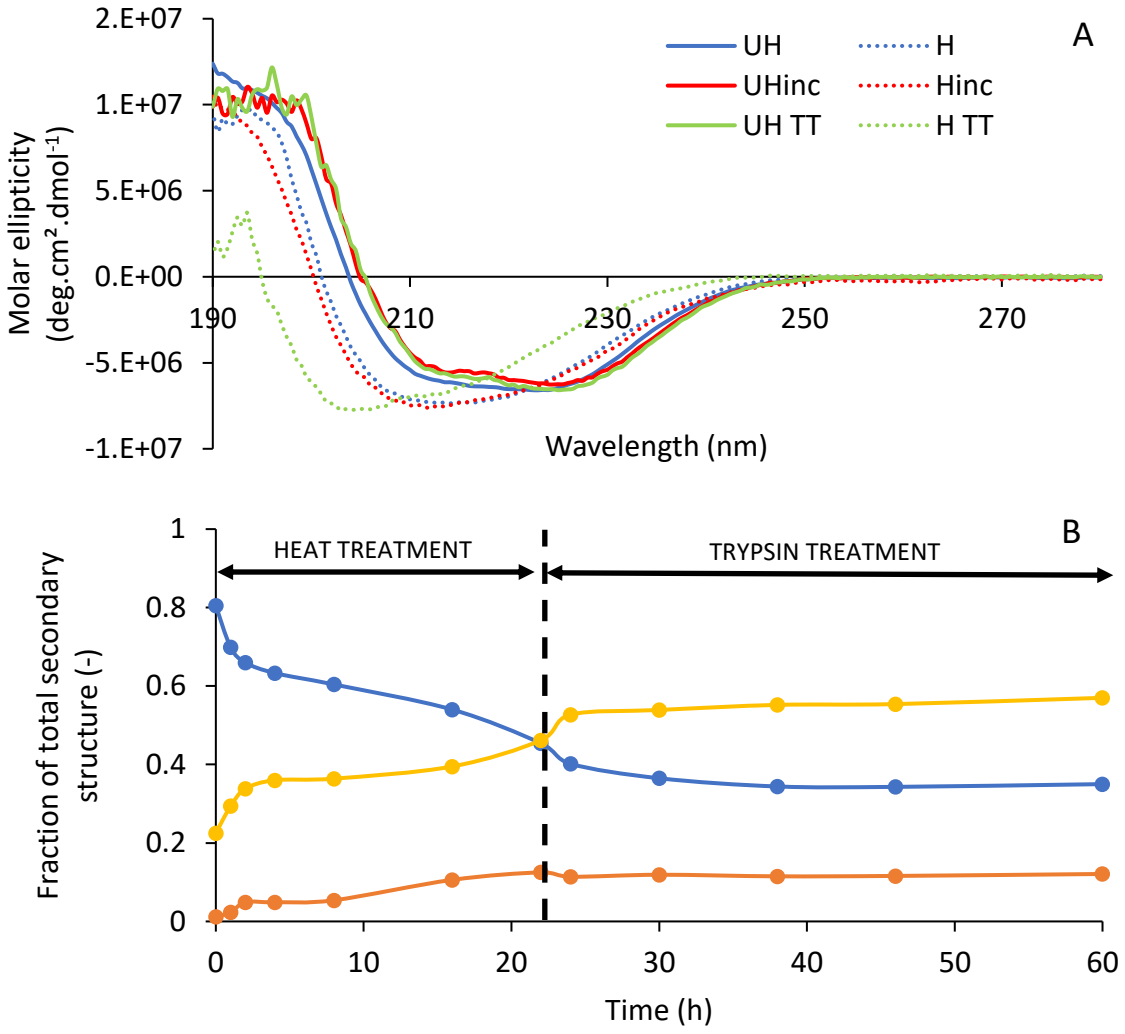

Figure 4: Circular dichroism (CD) spectra ranging from 190 to 280 nm for the different pretreated ovalbumin (OVA) dispersions (A). Samples are labelled as in section 2.2. Contribution of α-helix (blue), β-sheet (orange), β-turn and unordered (yellow) structures during heating at 78 °C (up to 22 h) and subsequent enzymatic treatment with trypsin (for 48 h) at 37 °C (B).

3.1.5. Size exclusion-high performance liquid chromatography

The SE-HPLC profiles of the different dispersions are shown in Figure 5 with monitoring of their UV absorbance and ThT fluorescence. UH OVA showed a large peak eluting at 10.0 min and a minor peak at 9.5 min, in accordance with the results of Monge-Morera et al. (2020) and Croguennec, Renault, Beaufils, Dubois, & Pezennec (2007). They assigned the large and small peak to OVA monomers and dimers, respectively. Furthermore, ThT fluorescence showed a negligible peak near 10.0 min. Upon further incubation (UHinc) or tryptic digestion (UH TT) of these UH OVA dispersions, alterations were detected neither in UV absorbance nor in ThT fluorescence (Figure S2).

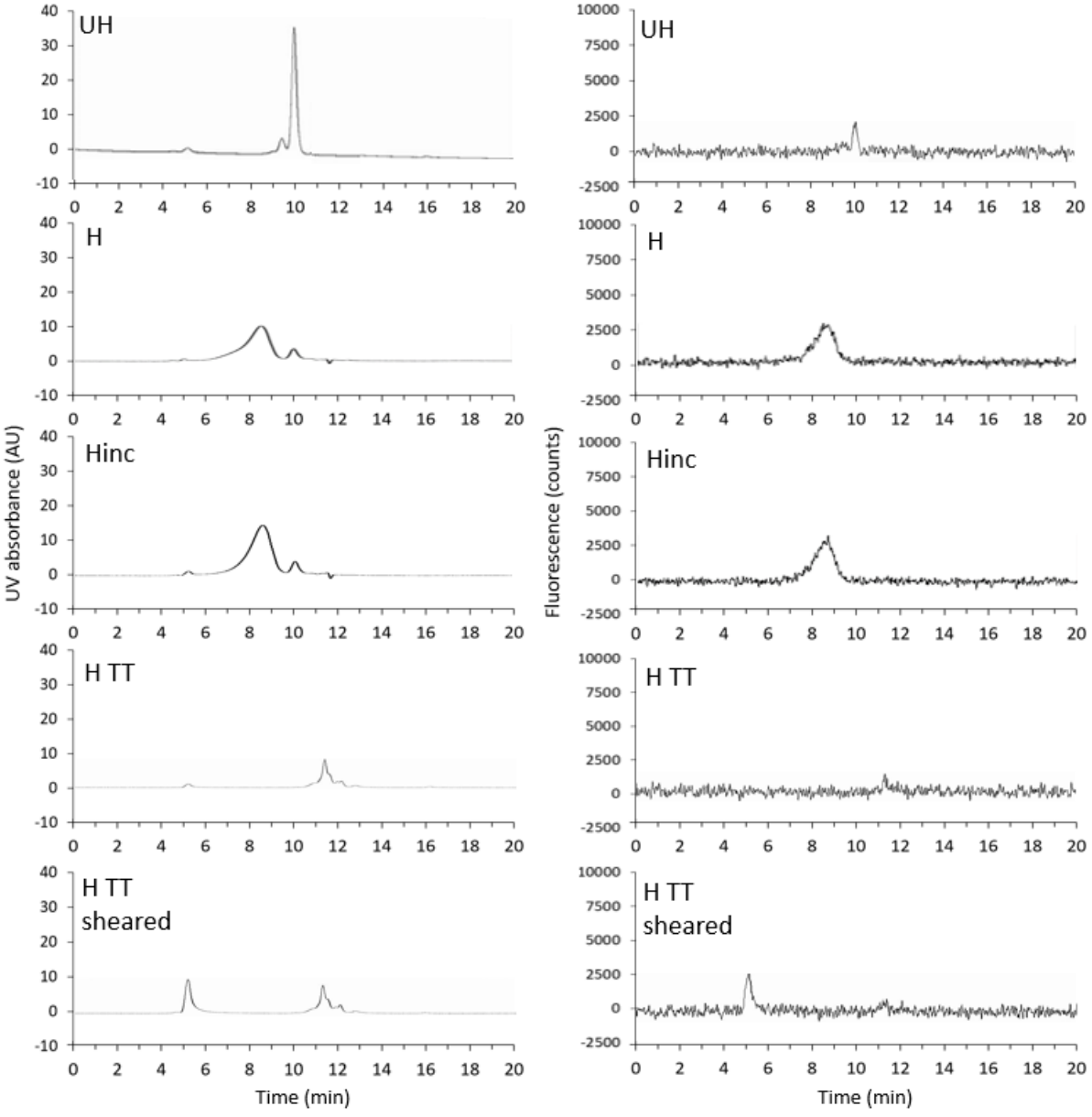

Figure 5: Size exclusion- high performance liquid chromatography (SE-HPLC) profiles monitored by (A) UV absorbance (280 nm) and (B) Thioflavin T (ThT) fluorescence (excitation at 440 nm, emission at 480 nm) measurements of different ovalbumin (OVA) dispersions. The samples were labelled as described in section 2.2. H TT sheared samples consisted of heated (78 °C for 22 h) and trypsin treated (8.0 µL trypsin solution per mL protein dispersions; incubation at 37 °C for 48 h) OVA dispersions subjected to 1 min microfluidizer treatment at 560 bar.

The UV absorbance profile of H OVA was different from that of UH OVA. Between 9.5 and 10.0 min, only a small peak was found, suggesting that the monomer and dimers were for the most part no longer present. In contrast, a novel broad peak eluting between 7.0 and 9.0 min was found which had a large ThT fluorescence signal, thus suggesting the presence of ALFs. The similar profiles of the Hinc OVA sample revealed that little if any structural changes occurred upon incubation at 37 °C. Lastly, the H TT OVA sample showed a negligibly small peak near 5.0 min and a broader one between 10.8 to 12.5 min. Whereas the peak at 5.0 min indicated the presence of larger ALFs, its area was too low for ThT fluorescence to be detected. Furthermore, H TT OVA sample also showed a shift towards longer elution times (peak around 10.8 to 12.5 min) indicating the presence of structures smaller than the native protein. As such, it was clear that the additional trypsin treatment formed peptides.

As TEM analysis revealed large fibrillar structures and the peak at 5 min only showed a small contribution, it follows that a large number of proteins present in the sample were not detected, indicating that they were so large that they were withheld during the prior filtration step. To confirm the absence of ALFs due to their removal during filtration, the H TT OVA sample was submitted to 60 s microfluidization treatment (at 560 bar) using a microfluidizer type M110S (Microfluidics, Lampertheim, Germany) in order to break down the long ALFs as previously also done by Oboroceanu et al. (2011) for WPI ALFs. The resulting UV absorbance chromatogram (Figure 5) revealed that the peak between 5.0 and 7.0 min was indeed significantly higher than for H TT OVA, thus proving the presence of smaller ALFs after microfluidization.

3.1.6. Quartz crystal microbalance with dissipation

The presence of peptides was further researched using QCM-D. As the adsorption kinetics in this technique rely mainly on diffusion-driven interactions (Setiowati et al., 2021), it seems logical that peptides would adsorb more rapidly on the coated sensors than proteins. During the first 25 min, milliQ water was pumped over the coated sensors to obtain a stable baseline. Afterwards, the tubes were changed to the corresponding 0.1% protein dispersions. All of them showed a decreased frequency and increased dissipation. These changes indicated that proteins were adsorbed to the sensors, although the changed density and viscosity of the liquid phase could also be (partly) responsible for this effect. Afterwards, demineralized water pumped over the sensors removed all non-adsorbed structures and ensured that the liquid had the same density and viscosity as during the baseline determination. As such, the final rinsing step did again lower the dissipation, whereas the frequency was increased. Hence, the corresponding frequency and dissipation shifts of UH (Figure 6A-B), H (Figure 6C-D) and H TT (Figure 6E-F) OVA were monitored.

The UH OVA and H OVA patterns showed a similar behavior. The dissipation after final rinsing showed a value below 1.10^{-6}, implying that a rather rigid layer had been formed. The latter was further sustained by the fact that all normalized frequency curves coincided during the rinsing step. The Sauerbrey formula was used to calculate the adsorbed mass from the normalized frequency shift of the different overtones. The calculated masses were not significantly different ($p = 1.00$) and were 1.83 ± 0.21 mg/m² and 1.89 ± 0.33 mg/m² for UH OVA and H OVA, respectively. These values are in the same order of magnitude as found for WPI (Setiowati, 2018), and typical for adsorbed protein monolayers (Tcholakova, Denkov, Ivanov, & Campbell, 2002; Tcholakova, Denkov, Sidzhakova, Ivanov, & Campbell, 2003). As both masses were similar, it is suggested that mainly unfolded or folded OVA was adsorbed, being the smallest common structures present in both samples. In contrast, H TT OVA showed a lower frequency shift than the other dispersions. The resulting calculated adsorbed mass

was only 0.74 ± 0.29 mg/m² and significantly lower than noted for both UH OVA and H OVA (p = 0.00). The corresponding dissipation also showed a lower value than the other dispersions, suggesting that an even more rigid layer was obtained and thus also that the adsorbed fraction in H TT OVA differed from those in UH OVA and H OVA. The lower adsorbed mass and higher rigidity suggested the presence of very small structures. Earlier, Dalgleish & Leaver (1991) showed that trypsin treatment of β-casein reduced the thickness of the absorbed layer. Hence, the QCM-D data confirmed the presence of non-fibrillogenic peptides which diffused more rapidly to the coated sensor interface. Unfortunately, the presence of large ALFs could not be confirmed by this technique. To better understand the adsorption properties of the present ALFs, the peptides need to be removed prior to analysis.

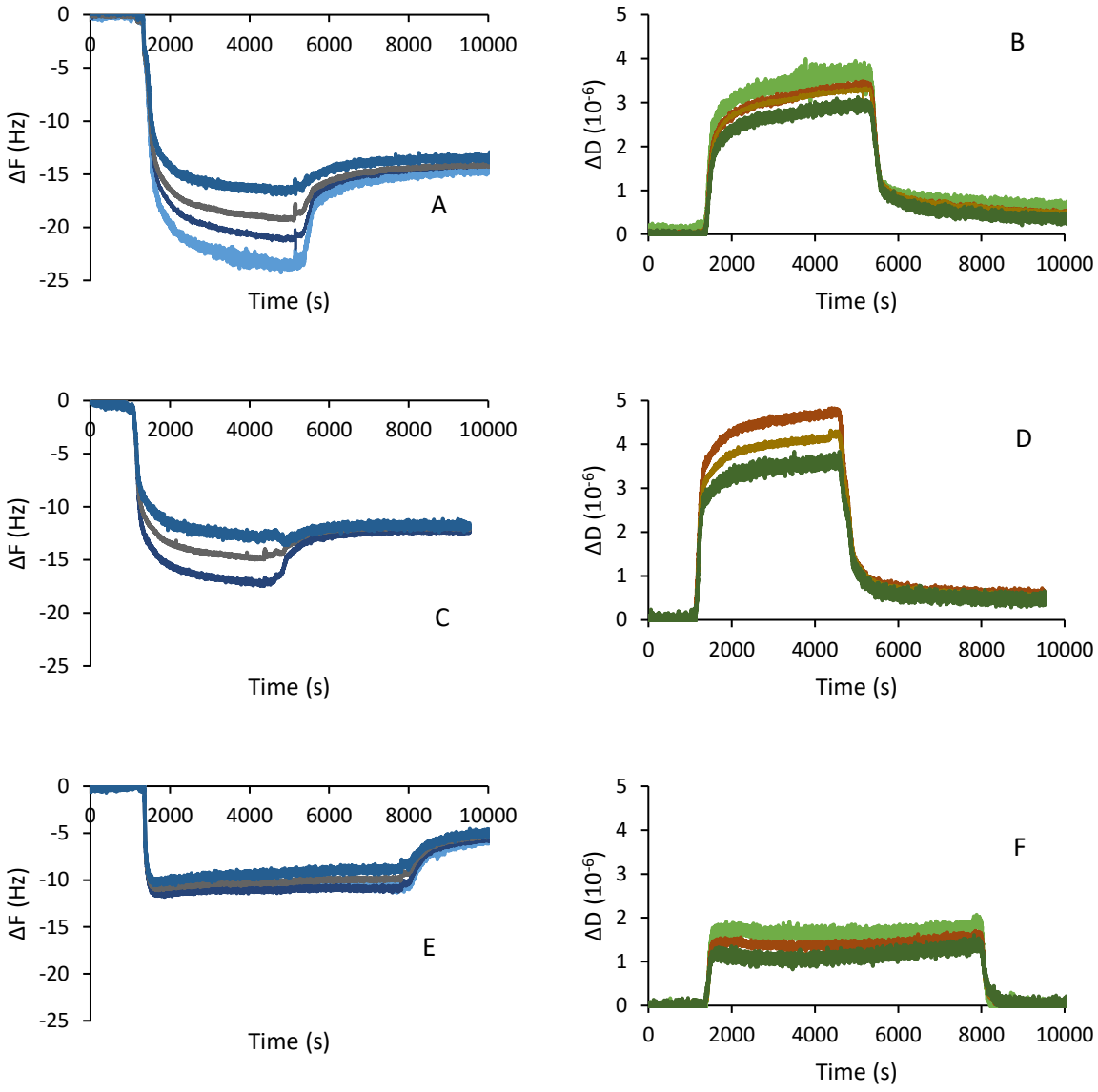

Figure 6: Frequency (A, C, E) and dissipation (B, D, F) shifts of (part of) overtones 5,7,9 and 11 of 0.01% (w/v) unheated (A, B), heated (C, D) and trypsin treated heated (E, F) ovalbumin (OVA) dispersions.

3.1.7. Viscosity

As a result of tryptic digestion and heat treatment, it was visually observed that the resultant H TT OVA dispersions formed transparent, gel-like textures. Rotational viscometry was performed in order to quantify the viscosity differences between all dispersions. An overview of the consistency coefficients

of all dispersions is provided in Table 1. The viscosity of the UH OVA sample was only slightly higher than that of pure water and further incubation with (UH TT) or without (UHinc) trypsin did not influence it, as expected from the above results. Furthermore, as a result of heating, the H OVA sample had a slightly higher viscosity than the UH OVA dispersion. This could be related to the presence of larger aggregates, either amorphous or fibrillar, in the former. Nevertheless, H OVA samples still had a liquid appearance. Further incubation of these H OVA samples did not lead to a significant increase in viscosity (Hinc OVA). However, similar incubation in the presence of trypsin resulted in a higher viscosity. The visual observation of such transparent gel structure has, to the best of our knowledge, not been mentioned before. However, increased viscosity upon fibrillation has already been observed after heating whey (Mohammadian & Madadlou, 2016; Mohammadian, Salami, Emam-Djomeh, Momen, & Moosavi-Movahedi, 2018) and rice (Zhang & Huang, 2014) proteins at acidic pH.

Table 1: Overview of the consistency coefficient of different heated and/or enzymatically treated dispersions containing 2.0% ovalbumin (OVA). Labelling of the samples was similar as explained in section 2.2. There are no statistical differences between samples with the same letter (95% confidence interval). The samples were labelled as described in section 2.2.

Sample	*Consistency coefficient (mPa.s)*
UH OVA	1.33 ± 0.13a
H OVA	2.52 ± 0.20b
UHinc OVA	1.49 ± 0.17a
Hinc OVA	2.59 ± 0.19b
UH TT OVA	1.39 ± 0.04a
H TT OVA	4389 ± 172c

According to Loveday, Rao, Creamer, & Singh (2009), β-lg samples containing longer ALFs as a result of heat treatment at pH 2.0. resulted in higher gel strength than did similar samples treated at pH 7.0. The latter rather contained small, worm-like fibrils. As such, the increased fibril length at pH 2.0 as a consequence of prior hydrolysis into peptides enabled the formation of longer ALFs and easier entanglement, which then likely was responsible for the increased viscosity. This probably also held for the H TT OVA dispersions considered here, as they also contained ALFs with a longer fibril length than did the H OVA samples. Of further note is that the AFM images of H TT OVA (Figure 3B) showed some entangled fibrillar structures.

3.1.8. Small amplitude oscillatory shear rheology

The increased viscosity observed for H TT OVA was further studied using small oscillatory shear experiments by performing a time sweep during 48 h whilst incubating H OVA dispersion with trypsin at 37 °C. The resultant graph (Figure 7B) showed that initially (0 h), G" was about 4 times as high as G'. This was in line with the liquid consistency of the H OVA sample as observed by rotational viscometry. However, a rapid increase of G' was observed around 14 h, eventually crossing G" at 16.9 h. This point was considered as the gelation time. During further incubation, a gel network was formed as its G' was higher than its G". Eventually, both moduli reached stable values (48 h), with G' being about 12 times higher than its corresponding G". The gelation could be related to the presence of (more) large and/or straight ALFs in H TT OVA than in H OVA. The latter contained small, flexible ALFs. Such behavior has already been described by Munialo, Martin, van der Linden, & de Jongh (2014). They observed that

gels containing long, rigid whey protein fibrils (formed by heating at 85 °C and pH 2.0 for 20 h) had higher strength than gels from similarly treated pea proteins containing curly fibrils.

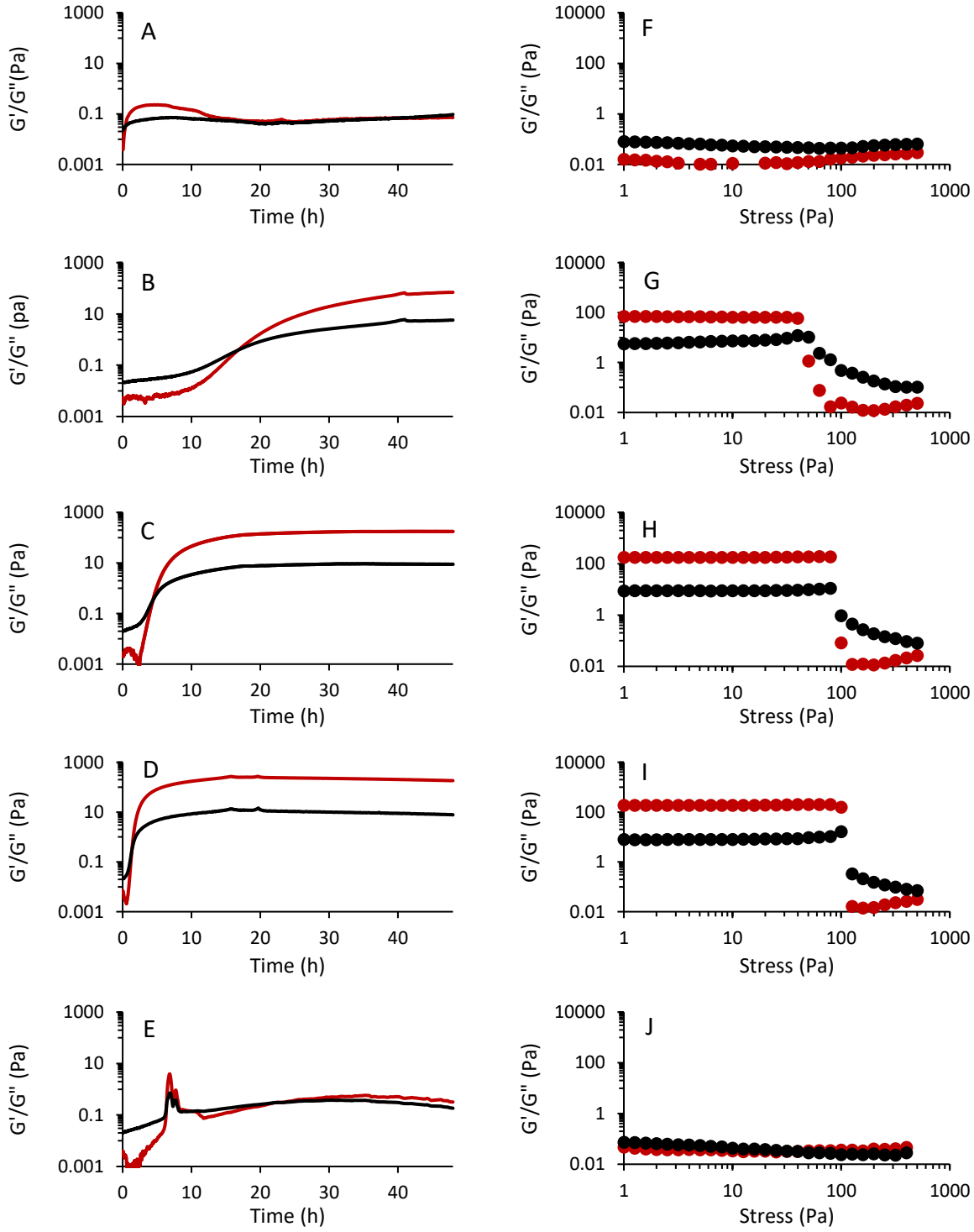

Figure 7: G' (red) and G" (black) measured by time sweeps (A-E) and amplitude stress sweeps (F-J) of 2.0% (w/v) heated (78 °C for 22 h) ovalbumin (OVA) dispersions which were incubated with 8 µl 2.0% trypsin solution per mL OVA dispersion for 48 h at 27 °C (A, F), 37 °C (B, G), 47 °C (C, H), 57 °C (D, I) and 67 °C (E, J). Time sweeps were carried out at a constant frequency and strain of 1 Hz and 0.01%, respectively. Amplitude sweeps were caried out at a constant frequency of 1 Hz.

The plots of G' and G" as a function of oscillatory stress (amplitude sweep) are depicted in Figure 7G. The LVR was considered up to an oscillatory stress of 30 Pa. The experimental time sweep and frequency sweep (i.e. oscillating stress of 0.5 Pa) conditions were thus situated in the LVR. Within this LVR, the H TT OVA dispersion behaved as a viscoelastic gel, as the G' remained larger than G". The average elastic modulus within the LVR (G'_{LVR}) had a value of 67.8 Pa. Furthermore, the gel destruction point (at which G' is lower than 0.9 times G'_{LVR}) during the amplitude sweep was around 38 Pa and a measure for the gel strength. The frequency sweep (Figure S3) provided information on the gel structure and strength when increasing deformation velocity. It was clear that the physical gel structure remained intact during the whole frequency range. Both G' and G" remained more or less constant, suggesting the formation of a strong gel network (Clark & Ross-Murphy, 1987). Under these conditions, G' was about 20 times higher than G". Furthermore, the elastic modulus and frequency (f) could be related according to the equation:

$$\log G' = n.\log f + K$$

With n being a measurement of the viscoelasticity (0 is pure elastic, higher value implies more viscous) and K a constant value. With our observations, this equation yielded an n-value of 0.05, suggesting the formation of an almost completely elastic gel.

Gelation was accompanied with some textural changes. Several authors claimed an increase in ThT fluorescence of protein-free dispersions when increasing the viscosity of the medium (Kuzmitskii & Stepuro, 2017; Stsiapura et al., 2008; Sulatskaya, Sulatsky, Antifeeva, Kuznetsova, & Turoverov, 2019). ThT fluorescence is based on deactivation of the excited state after excitation at 440 nm. In a free, unbound form, ThT can lose the excited state due to intramolecular twisting of the bond between its benzothiazole ring and aminobenzoyl ring (Amdursky, Erez, & Huppert, 2012; Kuzmitskii & Stepuro, 2017). However, the specific binding to cross β-sheet structures disables this twisting and the excited state is therefore lost due to fluorescence (480 nm). As an increased viscosity also partially disables the intermolecular twisting within the thioflavin T structure, an increased ThT fluorescence is obtained. Nevertheless, we here observed a decrease in relative ThT fluorescence upon trypsin incubation (and thus increased viscosity). It is hence suggested that the increased fluorescence due to the higher viscosity was lower than the loss in fluorescence due to insufficient accessibility of ThT towards the cross β-sheet structures due to gelation, resulting in a net decrease in relative ThT fluorescence.

The occurrence of transparent gels due to ALF formation is rare under neutral pH conditions, as these mainly give rise to small, worm-like fibrils (Monge-Morera et al., 2020). As such, these gels show a high potential for food applications. In section 3.2, the formation of trypsin-induced ALF gels is further studied in an effort to increase gel strength and accelerate gel formation.

3.2. Characterization of gels made from enzyme treated ovalbumin and optimization of their formation

3.2.1. Influence of incubation temperature on gelation

In a first attempt to accelerate the gelation and/or increase the gel strength, the incubation temperature during trypsin treatment was varied from the 37 °C considered above, which itself was based on Monge-Morera et al. (2020). Interestingly, the optimum temperature for trypsin activity at neutral pH is between 60 and 70 °C (Lambré et al., 2021). Dallas Johnson, Clark, & Marshall (2002)

observed increasing trypsin kinetics up to a temperature of 55 °C but did not include higher incubation temperatures in their experiments. In the present work, trypsin incubation temperatures varying between 27 °C and 67 °C were evaluated.

First, tryptic digestion of H OVA at 27 °C (Figure 7A) showed that during the time sweep G" remained larger than or similar to G' except for a small overshoot between 2 and 10 h. The latter did not indicate gelation as G' rapidly decreased again and did not remain several orders of magnitude higher than G". Furthermore, the corresponding frequency sweep (Figure S3) showed larger moduli when increasing the frequency. This corresponded with an n-value of 1.14, which confirmed the liquid consistency. Finally, the corresponding amplitude sweep (Figure 7F) showed a G" larger than G', indicating the absence of a gel network.

As already discussed in section 3.1.8, enzymatic treatment at 37 °C resulted in a gelation time of 16.9 h. It is clear from Figures 7C-D that an increase in incubation temperature to 47 °C and 57 °C resulted in reduced gelation times (4.5 h and 1.4 h, respectively). Gelation thus occurred more rapidly when incubating H OVA with trypsin at higher temperatures. Furthermore, the n-values derived from data collected in the frequency sweeps (Figure S3) were 0.03 for both samples incubated at 47 and 57 °C, indicative of the formation of strong elastic gel networks. The G' values for both conditions were almost equal and therefore the G' marks of the sample incubated at 47 °C (solid red triangles) were depicted under those of the sample incubated at 57 °C (solid green triangles), which explains the absence of the former in Figure S3. The gel was further characterized by the amplitude sweeps of both conditions (Figure 7H-I). The strength of the gels (expressed as G'_{LVR}) also increased in the order 68 Pa (37 °C), 179 Pa (47 °C), and even 186 Pa (57 °C). Furthermore, the stress at which the gel structure was disrupted, also increased from 38 Pa (37 °C) to 76 Pa and 100 Pa as a result of tryptic incubation at 47 and 57 °C, respectively. As such, increasing the incubation temperature did not only result in more rapid gelation, but also in higher gel strengths.

Lastly, including the time sweep data of the H OVA sample which had been enzymatically treated at 67 °C in Figure 7E again revealed the absence of a clear gel network as G' and G" were of a similar magnitude. The data also seemed more noisy, especially near 5 to 10 h of incubation. The latter probably corresponded with insufficient prevention of evaporation during incubation for two days at 67 °C even if a solvent trap had been used. Nevertheless, it is suggested that tryptic incubation under these conditions can further reduce the gelation time and result in strong gels. However, during the time frame shorter than that at which a gel is formed at 57 °C (1.4 h), G' remained clearly lower than G", indicative of its liquid consistency. The outcomes of the frequency sweep (Figure S3, showing an n-value of 1.9) and the amplitude sweep (Figure 7J, showing G' lower than G") confirmed the above as did the visual observation of a fluid character when removing the sample after rheological measurements.

3.2.2. Influence of preheating temperature on gelation

In addition to studying gelation as a function of the incubation temperature, the impact of deviations of the preheating temperature from 78 °C, as used above and claimed to be optimal for OVA ALF formation (Alting et al., 2004) was also studied. At its denaturation temperature (84.5 °C), OVA favors the formation of amorphous aggregates (Arnaudov & de Vries, 2005; Ow & Dunstan, 2013). Whereas H OVA, which contained a significant number of amorphous aggregates, did not gel, further breakdown of the aggregates and (partial) self-assembly of the resulting peptides into long ALFs during enzymatic treatment resulted in gelation of H TT OVA.

It seems that, when present, amorphous aggregates were removed upon tryptic digestion. The heating temperature has an impact on the formation of amorphous aggregates and hence on the gelation after enzymatic treatment. Whereas at lower heating temperatures less random aggregates are formed, it may require less time for trypsin to hydrolyze them into peptides. In contrast, heating at higher temperatures may produce more random aggregates which can be hydrolyzed into peptides and subsequently form ALFs. Here, preheating temperatures varying between 58 °C and 88 °C were applied.

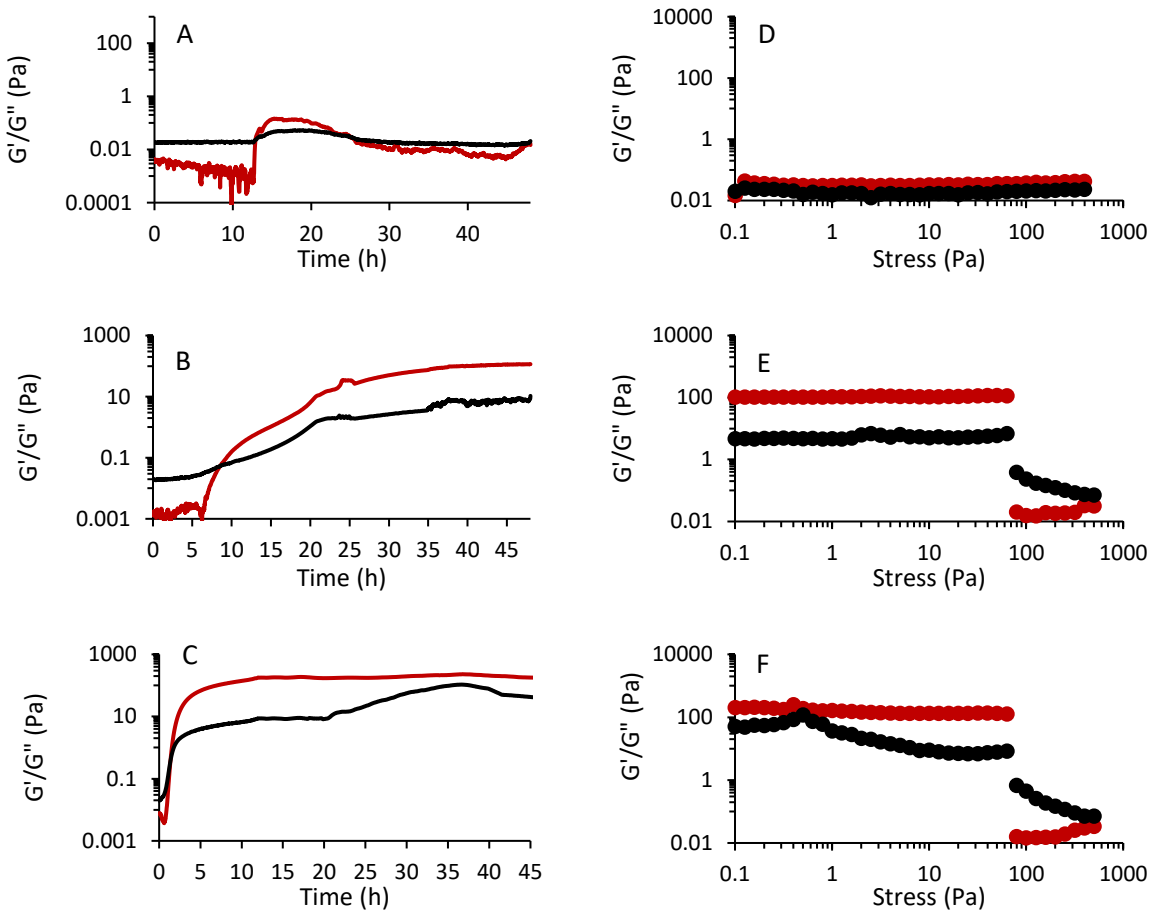

Figure 8: G' (red) and G" (black) measured by time sweeps (A-C) and amplitude stress sweeps (D-F) on 2.0% (w/v) heated ovalbumin (OVA) dispersions for 22 h at 58 °C (A, D), 68 °C (B, E) and 88 °C (C, F) which were incubated with 8 µl 2.0% trypsin solution per mL OVA dispersion for 48 h at 57 °C. Time sweeps were performed at a constant frequency and strain of 1 Hz and 0.01%, respectively. Amplitude sweeps were carried out at a constant frequency of 1 Hz.

Preheating at 58 °C did not result in gelation as the corresponding time sweep (Figure 8A) showed no dominating G' at the end of the incubation. Furthermore, the frequency sweep (Figure S4) showed a linear increase with n = 2.1 and the amplitude sweep (Figure 8D) indicated almost equal G' and G" over the total stress range, confirming the absence of a gel. Therefore, it is suggested that preheating OVA dispersions at 58 °C resulted in insufficient aggregate formation for assembly into ALFs.

Preheating at 68 °C did result in gelation (Figure 8B) six times later (8.5 h) than when preheating at 78 °C (1.4 h). This suggested that the lower preheating temperature resulted less in formation of ALFs

capable to entangle and induce gelation probably because of the presence of less amorphous aggregates at the lower temperatures. Furthermore, the reduced preheating temperature reduced the extent of protein unfolding resulting in non-aggregated OVA which was trypsin resistant. Not only did gelation at 68 °C occur later, the resultant gels were also weaker as revealed by the lower stress at which they started to break (63 Pa) than those preheated at 78 °C (100 Pa). Furthermore, the amplitude sweep of the H TT OVA samples preheated at 68 °C and 78 °C showed G'_{LVR} readings increasing in that order (106 Pa and 186 Pa, respectively).

Preheating at 88 °C resulted in a gelation time similar to that of the samples preheated at 78 °C (1.4 h). The resultant gels were stronger (G'_{LVR} of 126 Pa) than when preheating was executed at 68 °C, but still of significantly lower strength than when it had been done at 78 °C. Furthermore, when preheating had been done at either 88 °C or 68 °C, the resultant gels broke at similar stresses (63 Pa), while those formed when preheating had been done at 78 °C broke at 100 Pa.

It was thus shown that pretreatment at 78 °C resulted in an optimal composition of fibrillar structures and amorphous aggregates to rapidly create the strong gels.

3.2.3. Design of experiments: influence of protein concentration and trypsin quantity on gelation

After optimization of both preheating and incubation temperature, further optimization of the gelation procedure was performed by varying both the protein concentration (2.0-3.0-4.0%) and the trypsin quantity added to the protein dispersions (8-16-24 µL per mL OVA dispersion). To simultaneously vary both factors, a DOE was performed. An I-optimal response surface design was constructed for both gelation time, G'_{LVR} and σ* (Figure S5-7). As such, interaction effects between both factors could be deduced, using only a limited number of samples.

An overview of the different sample conditions and their resulting gelation time, G'_{LVR} and σ* is given in Table 2. The gelation time measured by rheometric analysis varied between 0 h (sample 12) and 1.58 h (sample 4). The corresponding response surface design and prediction plots are depicted in Figure 9. First, the surface plot for the gelation time (Figure 9A) only included the negative linear effects of OVA concentration ($p = 0.01$) and trypsin quantity ($p = 0.00$). In general, the gelation time increased when the OVA concentration and/or the trypsin quantity were decreased. This negative linear effect of OVA concentration is in line with the observation by Alting et al. (2004) that decreasing the WPI (9.0% to 3.0%) and OVA (5.0% to 2.0%) concentrations delayed the time at which an initial increase in G' and thus gelation occurred. In the present case, higher OVA concentrations may have resulted in particulate gelation during the preheating step which would have been undesired in view of the scope of this research. To the best of our knowledge, no earlier publications on the effect of enzyme concentration on ALF containing gels are available. However, it seems logical that increasing the concentration of the component which induces gelation accelerates it. Ako et al. (2010) earlier showed more rapid salt-induced gelation at higher ionic strength. Furthermore, increasing the trypsin quantity (coefficient of -0.43) had a slightly higher impact on the gelation time than did a similar increase in OVA concentration (coefficient of -0.34). As such, it is believed that adding more trypsin to enable the formation of longer ALFs was slightly more important (due to a larger negative coefficient) to increase the velocity of gelation than having higher protein concentrations. This seems logical as gelation was

induced by adding trypsin rather than by increasing the OVA concentration. Furthermore, the quadratic and the interaction effects of both factors did not contribute significantly to the final model.

The linear surface plot showed a predicted minimum gelation time at 4.0% OVA and 24 µL trypsin solution per mL OVA dispersion. This corresponded with the lowest actual gelation time, as measured by the time sweep analysis. The gelation time measured was 0 h as G' was already dominant over G" at the start of the time sweep (Figure S5.12). This suggested that adding a quantity of 24 µL trypsin solution per mL 4.0% H OVA dispersions would induce immediate gelation without the necessity to incubate at 57 °C. It is of note here that prior to the time sweep, a conditioning period of 5 min was applied to enable the sample to reach the incubation temperature. Nevertheless, when a similar trypsin treatment was performed in a water bath at 57 °C for 5 to 30 min, no gel could be seen by the naked eye. Also, Figure S5.10-12 (containing 4.0% OVA) revealed that G' at the start of time sweep measurements was already slightly higher than for samples containing 2.0% or 3.0% OVA. As such, preheating 4.0% OVA may already have increased the viscosity and thus G', which made it easier for the latter modulus to become dominating over G". Therefore, both observations suggested that the crossover point of G' and G" not necessarily implies the visual observation of a gel structure.

Table 2: Overview of the different ovalbumin (OVA) concentrations and trypsin quantities added for the different samples considered in the design of experiment (DOE) set-up together with their resulting gelation time (t_{gel}), elastic modulus in the linear visco-elastic region (G'_{LVR}) and oscillating stress at gel fracture (σ^*) after small oscillatory shear stress experiments, and the T_2 relaxation time, as measured by low resolution NMR. The latter consisted of a time sweep for 12 h at 57 °C at 1 Hz and 0.01% oscillating strain followed by an amplitude sweep at 1 Hz. Normalized factors are indicated between brackets.

Sample	OVA concentration (%)	Trypsin quantity (µL/mL OVA)	t_{gel} (h)	G'_{LVR} (Pa)	σ^* (Pa)	T_2 (ms)
1	2 (-1)	8 (-1)	1.42	186	100	451
2	2 (-1)	16 (0)	0.80	271	200	450
3	2 (-1)	24 (1)	0.57	277	200	434
4	3 (0)	8 (-1)	1.58	419	316	323
5	3 (0)	16 (0)	0.50	668	397	321
6	3 (0)	16 (0)	0.53	613	398	328
7	3 (0)	16 (0)	0.48	614	398	328
8	3 (0)	16 (0)	0.48	629	398	328
9	3 (0)	24 (1)	0.33	713	399	328
10	4 (1)	8 (-1)	0.48	829	494	250
11	4 (1)	16 (0)	0.26	917	286	256
12	4 (1)	24 (1)	0	938	251	253

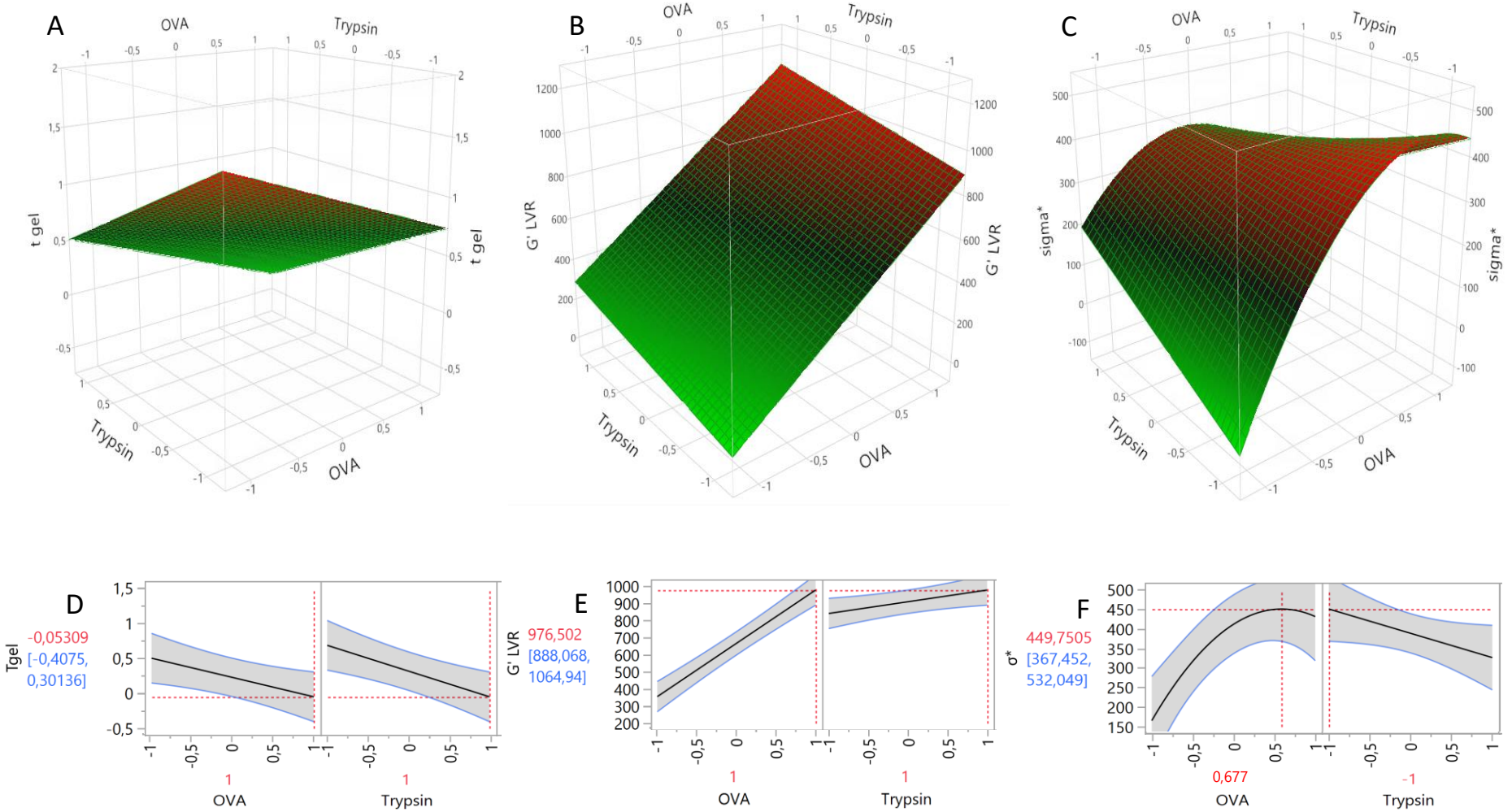

Figure 9: Response surface plots (A-C) and prediction profiles (D-F) of the predicted equations for gelation time (t_{gel}, A, D), elastic modulus in the linear visco-elastic region (G'_{LVR}, B, E) and oscillating stress at gel fracture (σ*, C, F) as a function of ovalbumin (OVA) concentration and trypsin quantity. These equations were predicted by fitting to data after small oscillatory shear stress experiments of the samples considered in the design of experiment and are expressed in function of the normalized factor values.

Furthermore, the G'_{LVR} values varied between 186 Pa (sample 1) and 938 Pa (sample 12). This indicated a significantly increased G'_{LVR} when both factors were maximized, as confirmed by the corresponding surface design (Figure 9B). The latter surface plot and the prediction plot (Figure 9E) revealed that G'_{LVR} was positively influenced by the linear effects of both OVA concentration ($p = 0.00$) and trypsin quantity ($p = 0.01$). The highest G'_{LVR} was obtained at maximum OVA concentration and trypsin quantity. Furthermore, increasing the OVA concentration (coefficient of 325) resulted in a higher increase in G'_{LVR} than a similar increase in trypsin quantity (coefficient of 82). This indicated that the higher gel strength determined by G'_{LVR} was influenced more by the protein concentration than by the quantity of trypsin. The large effect of the protein concentration on G'_{LVR} was in accordance with results of Munialo et al. (2014) and Alting et al. (2004). They respectively claimed that increasing pea protein and OVA concentrations from 4.0% to 8.0% and from 2.0% to 5.0%, respectively, resulted in a threefold increase in G'_{LVR}. In the latter case, this was suggested to be the consequence of more junctions being created between protein structures (Alting et al., 2004). This can easily be related to more entanglement between ALFs as a result of higher quantities thereof. Again, none of the quadratic or interaction effects were statistically significant. To be complete, the gel rigidity (G*) was similar to G'_{LVR} due to the dominating value of the latter over G''_{LVR}. As such, the rigidity was highly linked to the upper-mentioned relationship between OVA concentration, trypsin quantity and $G'_{LVR.}$

Additional T_2 relaxation measurements were performed to understand the water-binding capacity of the different gel systems considered in the DOE (Table 2). The higher the protein concentration was, the shorter the T_2 relaxation time was and thus the more bound water was present. In contrast, the impact of increased trypsin quantity (at constant OVA concentration) was limited. As such, these data were largely in line with those obtained for G'_{LVR}, suggesting that stronger gels had a higher water-binding capacity and that especially the OVA concentration was a determining factor.

Finally, the data for σ* varied between 100 Pa (sample 1) and 494 Pa (sample 10). The critical stress at which the gel started to break could not be explained by a linear model as shown in Figure 9C. Next to the linear effect of OVA concentration ($p = 0.01$), also the interaction ($p = 0.06$) and the quadratic ($p = 0.01$) effects of OVA concentration were significant. The linear effect of trypsin quantity was not significant ($p = 0.28$) but could not be removed due to the significant (higher order) interaction effect. The corresponding prediction plot (Figure 9F) showed a maximum σ* at an OVA concentration of 3.7% and 8 µL trypsin solution per mL OVA dispersion. The positive linear effect of OVA concentration (coefficient of 89) revealed that higher protein concentration maintained the gel structure up to a higher oscillating stress. Furthermore, the large positive effect of the OVA concentration was reduced at higher concentrations due to the negative quadratic effect (coefficient of -129). This suggested that increasing the OVA at low concentrations positively influenced the σ*, whereas at high concentrations this had a negative effect, as could be deduced from Figure 9F.

The negative interaction term (coefficient of -86) also reduced the σ*. As such, the overall influence of both factors on σ* was more than just the sum of both separate factors. Whereas the linear effect of OVA concentration was positive, the addition of more trypsin (coefficient of -10) diminished the critical stress at which the gels started to break. Nevertheless, comparison with the actual data showed that trypsin quantity only had an impact for the samples at 4.0% OVA, explaining why the linear factor for trypsin quantity was not significant. In fact, for 2.0 and 3.0% OVA, positive effects were observed. However, the large decrease in σ* from sample 10 (494 Pa) to sample 11 (286 Pa) and 12 (251 Pa) was more profound than the small increases between samples 4 (316 Pa) and 9 (399 Pa) and between

samples 1 (100 Pa) and 3 (200 Pa). It is believed that the gels of samples 11 and 12 contained such high OVA concentration that the large trypsin quantity resulted in too high levels of non-fibrillogenic peptides which imposed limits on the extent of entanglement. As a result, the limited gelation created voids resulting in reduced gel strength. The latter may well explain the negative interaction term in this model. Nevertheless, the brittleness [expressed by tan(ϕ)] which was between 0.04 and 0.06 suggested no significant differences between the samples.

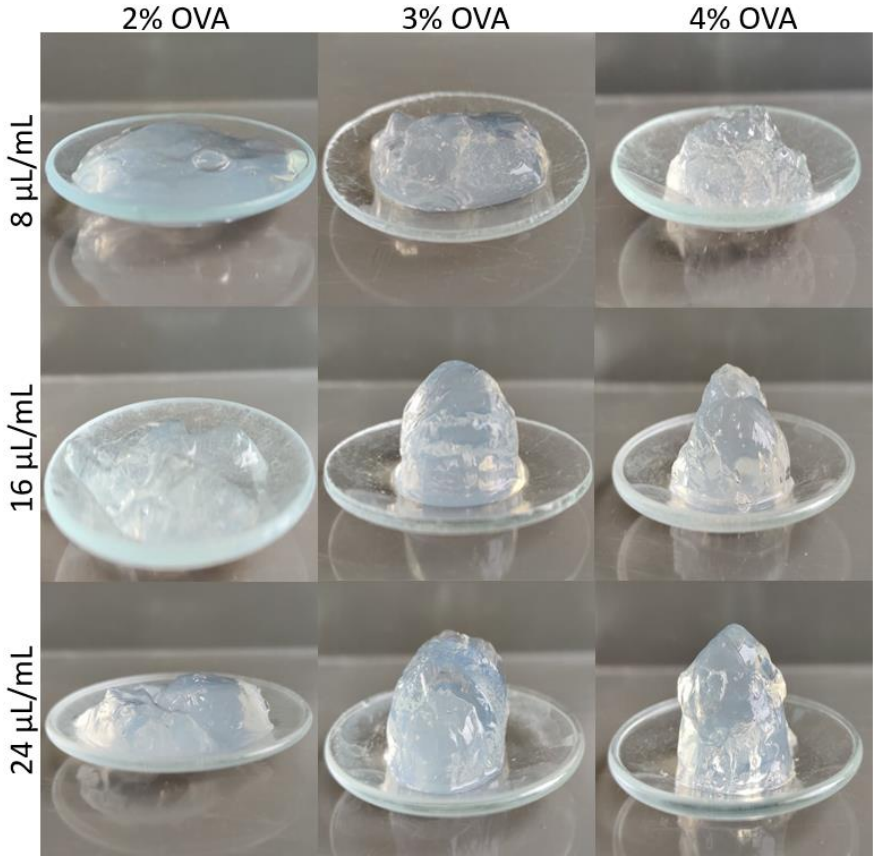

Figure 10: Visual representation of the samples obtained after heat (78 °C for 22 h) and trypsin (57 °C for 7 h) treatment at the different conditions selected for the design of experiment (DOE) set-up. The latter considered two variables: the ovalbumin (OVA) concentration which varied between 2.0% and 4.0%, and the trypsin quantity which was between 8 and 24 µL per mL of OVA dispersion.

The H TT OVA gels obtained after 7 h trypsin incubation in a water bath are shown in Figure 10. Based on the outcome of the time sweep data of these samples (Figure S5), 7 h incubation was assumed to suffice to obtain transparent gels for all conditions. Gels containing 2.0% OVA were still able to flow under gravitational forces, whereas increasing the trypsin quantity resulted a slight increase in rigidity. Nevertheless, the increased rigidity did not prevent the gel from settling under gravitational forces when poured on glass. Similar observations were made for 3.0% OVA gels when 8 µL trypsin solution had been added per mL OVA dispersion. However, increasing both OVA concentration to 3.0-4.0% and trypsin quantity to 16-24 µL trypsin solution per mL OVA dispersion resulted in self-standing gels.

4. Conclusions

We here studied the effect of heat and/or enzymatic treatment of OVA on the formation of ALFs and their morphology. Whereas heating of OVA (78 °C, 22 h) resulted in increased relative ThT and ANS fluorescence, indicating the presence of ALFs and high surface hydrophobicity, respectively, both

parameters decreased again when an additional enzymatic treatment was performed. However, other techniques revealed that the latter samples contained larger and more straight OVA ALFs than when OVA was only heated. Additionally, the enzymatic treated dispersions revealed that next to ALFs also peptides remained present. In contrast, the absence of ALF formation when performing a similar enzymatic treatment on UH OVA revealed that unfolded or aggregated protein structures were required to enable extensive hydrolysis. Hence, this confirmed the hypothesis by Lambrecht et al. (2019) that the amorphous aggregates formed during the prior heating step were hydrolyzed into peptides of which some could assemble into larger fibrillar structures.

H OVA and H TT OVA not only showed differences at microscale, but also different macroscopic properties as the latter showed a transparent gel-like texture. The latter was suggested to be due to entanglement of long OVA ALFs. Small oscillatory shear experiments revealed that a gel was formed after 17 h. Its G'_{LVR} was 68 Pa and it broke at a stress of 38 Pa (σ^*). Whereas this was a rather time-consuming process, the gelling procedure was successfully reduced to 1.4 h by increasing the incubation temperature during enzymatic treatment from 37 °C to 57 °C. The latter temperature was closer to the optimum enzyme temperature which remarkably enhanced the rate of hydrolysis. Additionally, these gels had a higher strength as compared to those formed at 37 °C.

Based on the above optimized temperature conditions, an experimental design was used to evaluate the effect of OVA concentration and trypsin quantity on the gel characteristics. As such, it was suggested that the highest OVA concentration (4.0%) combined with 24 µL trypsin solution per mL OVA dispersion resulted in the most rapid gelation and at the same moment also the highest gel strength (based on G'_{LVR}). As trypsin was the gel-inducing compound, it was likely that increasing its concentration would enhance gelation. Nevertheless, gels formed at the highest OVA and trypsin concentration already started breaking at a lower stress than when less trypsin was added, suggesting that extensive hydrolysis had a negative effect on the gel resistance to disruption.

Overall, it is clear that a combined heat and enzymatic treatment enabled the formation of transparent gels with various characteristics. Hence, the thus prepared OVA ALFs hold promise for improving different food formulations. Additionally, this gelation capacity may be beneficial for improving the creaming and coalescence stability of O/W emulsions with a high oil content, such as mayonnaises.

5. Acknowledgements

This work was part of the Strategic Basic Research project ProFibFun executed in close collaboration between Ghent University and KU Leuven, funded by the Research Foundation-Flanders (FWO, SBO grant S003918N, Brussels, Belgium). J.A. Delcour is the beneficiary of Methusalem excellence funding at the KU Leuven. The Switch laboratory is supported by the Flanders Institute for Biotechnology (VIB, grant no. C0401); KU Leuven; and the Fund for Scientific Research Flanders (FWO, grant I011220N). A.M.R. Huyst would gratefully like to acknowledge Prof. M. Van Troys and the Laboratory of Biomolecular Medicine (Faculty of Medicine and Health Sciences, Ghent University) for the use of the circular dichroism technique. L. Van der Meeren and A.G. Skirtach thank FWO (I002620N, G043219N) and BOF UGent (IOP 01/O3618, BAS094-18) for support.

Abalymov, A., Santos, C., Van der Meeren, L., Van de Walle, D., Dewettinck, K., Parakhonskiy, B., & Skirtach, A. (2021). Nanofibrillar hydrogels by temperature driven self-assembly: new structures for cell growth and their biological and medical implications. *Advanced Materials Interfaces*, *8*(15), 1–11. https://doi.org/10.1002/admi.202002202

Akkermans, C., van der Goot, A., Venema, P., van der Linden, E., & Boom, R. (2008). Properties of protein fibrils in whey protein isolate solutions: microstructure, flow behaviour and gelation. *International Dairy Journal*, *18*(10), 1034–1042. https://doi.org/10.1016/j.idairyj.2008.05.006

Ako, K., Nicolai, T., & Durand, D. (2010). Salt-induced gelation of globular protein aggregates: Structure and kinetics. *Biomacromolecules*, *11*(4), 864–871. https://doi.org/10.1021/bm9011437

Ako, K., Nicolai, T., Durand, D., & Brotons, G. (2009). Micro-phase separation explains the abrupt structural change of denatured globular protein gels on varying the ionic strength or the pH. *Soft Matter*, *5*(20), 4033–4041. https://doi.org/10.1039/b906860k

Alavi, F., Chen, L., & Emam-Djomeh, Z. (2021). Structuring of acidic oil-in-water emulsions by controlled aggregation of nanofibrillated egg white protein in the aqueous phase using sodium hexametaphosphate. *Food Hydrocolloids*, *112*(3), 106359. https://doi.org/10.1016/j.foodhyd.2020.106359

Alting, A., Weijers, M., de Hoog, E., van de Pijpekamp, A., Cohen Stuart, M., Hamer, R., … Visschers, R. (2004). Acid-induced cold gelation of globular proteins: effects of protein aggregate characteristics and disulfide bonding on rheological properties. *Journal of Agricultural and Food Chemistry*, *52*(3), 623–631. https://doi.org/10.1021/jf034753r

Amdursky, N., Erez, Y., & Huppert, D. (2012). Molecular rotors: What lies behind the high sensitivity of the thioflavin-T fluorescent marker. *Accounts of Chemical Research*, *45*(9), 1548–1557. https://doi.org/10.1021/ar300053p

Arnaudov, L., & de Vries, R. (2005). Thermally induced fibrillar aggregation of hen egg white lysozyme. *Biophysical Journal*, *88*(1), 515–526. https://doi.org/10.1529/biophysj.104.048819

Arnaudov, L., de Vries, R., Ippel, H., & van Mierlo. (2003). Multiple steps during the formation of β-lactoglobulin fibrils. *Biomacromolecules*, *4*(6), 1614–1622. https://doi.org/10.1021/bm034096b

Asgar, M., Fazilah, A., Huda, N., Bhat, R., & Karim, A. (2010). Nonmeat protein alternatives as meat extenders and meat analogs. *Comprehensive Reviews in Food Science and Food Safety*, *9*(5), 513–529. https://doi.org/10.1111/j.1541-4337.2010.00124.x

Astbury, W., Dickinson, S., & Bailey, K. (1935). The X-ray interpretation of denaturation and the structure of the seed globulins. *Biochemical Journal*, *29*(10), 2351–2360. https://doi.org/10.1042/bj0292351

Banerjee, S., & Bhattacharya, S. (2012). Food gels: gelling process and new applications. *Critical Reviews in Food Science and Nutrition*, *52*(4), 334–346. https://doi.org/10.1080/10408398.2010.500234

Barbut, S. (1995). Effect of sodium level on the microstructure and texture of whey protein isolate gels. *Food Research International*, *28*(5), 437–443. https://doi.org/10.1016/0963-9969(95)00034-8

Bolder, S., Hendrickx, H., Sagis, L., & van der Linden, E. (2006). Fibril assemblies in aqueous whey protein mixtures. *Journal of Agricultural and Food Chemistry*, *54*(12), 4229–4234. https://doi.org/10.1021/jf060606s

Chiti, F., & Dobson, C. (2006). Protein misfolding, functional amyloid, and human disease. *Annual Review of Biochemistry*, *75*(1), 333–366. https://doi.org/10.1146/annurev.biochem.75.101304.123901

Clark, A., & Ross-Murphy, S. (1987). Structural and mechanical properties of biopolymer gels. In *Biopolymers* (pp. 57–192). Berlin, Heidelberg: Springer Berlin Heidelberg.

Dalgleish, D., & Leaver, J. (1991). Dimensions and possible structures of milk proteins at oil–water interfaces. In E. Dickinson (Ed.), *Food Polymers, Gels and Colloids* (pp. 113–122). Cambridge: Woodhead Publishing. https://doi.org/https://doi.org/10.1533/9781845698331.113

Dallas Johnson, K., Clark, A., & Marshall, S. (2002). A functional comparison of ovine and porcine trypsins. *Comparative Biochemistry and Physiology - B Biochemistry and Molecular Biology*, *131*(3), 423–431. https://doi.org/10.1016/S1096-4959(01)00516-4

Emeson, E. E., & Kikkawa, Y. (1959). New features of amyloid found after digestion with trypsin. *Journal of Cell Biology*, *28*(3), 570–577.

Gao, Y., Xu, H., Ju, T., & Zhao, X. (2013). The effect of limited proteolysis by different proteases on the formation of whey protein fibrils. *Journal of Dairy Science*, *96*(12), 7383–7392.

Goos, P., & Jones, B. (2011). *Optimal design of experiments: a case study approach*. (Wiley, Ed.) (first edit). West Sussex. https://doi.org/10.1002/9781119974017

Gumus, C. (2018). Plant-based proteins: an alternative to synthetic emulsifiers. *International News on Fats, Oils and Related Materials*, *29*(5), 14–16. https://doi.org/10.21748/inform.05.2018.14

Harrison, R., Sharpe, P., Singh, Y., & Fairlie, D. (2007). Amyloid peptides and proteins in review. In S. G. Amara, E. Bamberg, B. Fleischmann, T. Gudermann, S. C. Hebert, R. Jahn, … R. Zechner (Eds.), *Reviews of Physiology, Biochemistry and Pharmacology* (pp. 1–77). Berlin, Heidelberg: Springer Berlin Heidelberg. https://doi.org/10.1007/112_2007_0701

Hatta, H., Kitabatake, N., & Doi, E. (1986). Turbidity and hardness of a heat-induced gel of hen egg ovalbumin. *Agricultural and Biological Chemistry*, *50*(8), 2083–2089.

Holm, N. K., Jespersen, S. K., Thomassen, L. V., Wolff, T. Y., Sehgal, P., Thomsen, L. A., … Otzen, D. E. (2007). Aggregation and fibrillation of bovine serum albumin. *Biochimica et Biophysica Acta - Proteins and Proteomics*, *1774*(9), 1128–1138. https://doi.org/10.1016/j.bbapap.2007.06.008

Hongsprabhas, P., & Barbut, S. (1996). Ca2+-induced gelation of whey protein isolate: Effects of pre-heating. *Food Research International*, *29*(2), 135–139. https://doi.org/10.1016/0963-9969(96)00011-7

Humblet-Hua, N., Scheltens, G., van der Linden, E., & Sagis, L. M. C. (2011). Encapsulation systems based on ovalbumin fibrils and high methoxyl pectin. *Food Hydrocolloids*, *25*(4), 569–576. https://doi.org/10.1016/j.foodhyd.2011.01.003

Huyst, A., Deleu, L., Luyckx, T., Buyst, D., Van Camp, J., Delcour, J. A., & Van der Meeren, P. (2022). Colloidal stability of oil-in-water emulsions prepared from hen egg white submitted to dry and/or wet heating to induce amyloid-like fibril formation. *Food Hydrocolloids*, *125*(6), 107450. https://doi.org/10.1016/j.foodhyd.2021.107450

Huyst, A., Deleu, L., Luyckx, T., Lambrecht, M., Van Camp, J., Delcour, J. A., & Van der Meeren, P. (2021). Influence of hydrophobic interfaces and shear on ovalbumin amyloid-like fibril formation in oil-in-water emulsions. *Food Hydrocolloids*, *111*(2), 106327. https://doi.org/10.1016/j.foodhyd.2020.106327

Ikeda, S., & Li-Chan, E. (2004). Raman spectroscopy of heat-induced fine-stranded and particulate β-

lactoglobulin gels. *Food Hydrocolloids*, *18*(3), 489–498. https://doi.org/10.1016/j.foodhyd.2003.07.003

Israelachvili, J. (2011). Special interactions: hydrogen-bonding and hydrophobic and hydrophilic interactions. In *Intermolecular and Surface Forces* (Third Edit, pp. 151–167). Cambridge: Academic Press. https://doi.org/10.1016/B978-0-12-375182-9.10008-9

Jansens, K., Lambrecht, M., Rombouts, I., Monge-Morera, M., Brijs, K., Rousseau, F., … Delcour, J. A. (2019). Conditions governing food protein amyloid fibril formation — part I : egg and cereal proteins. *Comprehensive Reviews in Food Science and Food Safety*, *18*(4), 1256–1276. https://doi.org/10.1111/1541-4337.12462

Jansens, K., Rombouts, I., Grootaert, C., Brijs, K., Van Camp, J., Van der Meeren, P., … Delcour, J. A. (2019). Rational design of amyloid-like fibrillary structures for tailoring food protein techno-functionality and their potential health implications. *Comprehensive Reviews in Food Science and Food Safety*, *18*(1), 84–105. https://doi.org/10.1111/1541-4337.12404

Kato, Y., Watanabe, K., Nakamura, R., & Sato, Y. (1983). Effect of pre heat treatment on tryptic hydrolysis of Maillard-reacted ovalbumin. *Journal of Agricultural and Food Chemistry*, *31*(2), 437–441. Retrieved from http://www.ncbi.nlm.nih.gov/pubmed/6853867

Kelly, S., Jess, T., & Price, N. (2005). How to study proteins by circular dichroism. *Biochimica et Biophysica Acta - Proteins and Proteomics*, *1751*(2), 119–139. https://doi.org/10.1016/j.bbapap.2005.06.005

Khurana, R., Coleman, C., Ionescu-Zanetti, C., Carter, S., Krishna, V., Grover, R., … Singh, S. (2005). Mechanism of thioflavin T binding to amyloid fibrils. *Journal of Structural Biology*, *151*(3), 229–238. https://doi.org/10.1016/j.jsb.2005.06.006

Knauer, M. F., Soreghan, B., Burdick, D., Kosmoski, J., & Glabe, C. G. (1992). Intracellular accumulation and resistance to degradation of the Alzheimer amyloid A4/β protein. *Proceedings of the National Academy of Sciences of the United States of America*, *89*(16), 7437–7441. https://doi.org/10.1073/pnas.89.16.7437

Krebs, M., Wilkins, D., Chung, E., Pitkeathly, M., Chamberlain, A., Zurdo, J., … Dobson, C. (2000). Formation and seeding of amyloid fibrils from wild-type hen lysozyme and a peptide fragment from the β-domain. *Journal of Molecular Biology*, *300*(3), 541–549. https://doi.org/10.1006/jmbi.2000.3862

Kroes-Nijboer, A., Venema, P., Bouman, J., & van der Linden, E. (2011). Influence of protein hydrolysis on the growth kinetics of B-lg fibrils. *Langmuir*, *27*(10), 5753–5761. https://doi.org/10.1021/la104797u

Kuzmitskii, V., & Stepuro, V. (2017). Triplet states of thioflavin T in fluorescent molecular rotor model. *Journal of Applied Spectroscopy*, *83*(6), 1031–1034. https://doi.org/10.1007/s10812-017-0402-x

Lam, R., & Nickerson, M. (2013). Food proteins: A review on their emulsifying properties using a structure-function approach. *Food Chemistry*, *141*(2), 975–984. https://doi.org/10.1016/j.foodchem.2013.04.038

Lambré, C., Barat Baviera, J., Bolognesi, C., Cocconcelli, P., Crebelli, R., Gott, D., … Chesson, A. (2021). Safety evaluation of food enzyme trypsin from porcine pancreas. *EFSA Journal*, *19*(6), 6637. https://doi.org/10.2903/j.efsa.2021.6637

Lambrecht, M., Jansens, K., Rombouts, I., Brijs, K., Rousseau, F., Schymkowitz, J., & Delcour, J. A. (2019). Conditions governing food protein amyloid fibril formation. part II: milk and legume

proteins. *Comprehensive Reviews in Food Science and Food Safety*, *18*(4), 1277–1291. https://doi.org/10.1111/1541-4337.12465

Lambrecht, M., Monge-Morera, M., Godefroidt, T., Vluymans, N., Deleu, L., Goos, P., … Delcour, J. A. (2021). Hydrothermal treatments cause wheat gluten-derived peptides to form amyloid-like fibrils. *Journal of Agricultural and Food Chemistry*, *69*(6), 1963–1974. https://doi.org/10.1021/acs.jafc.0c05868

Lambrecht, M., Rombouts, I., De Ketelaere, B., & Delcour, J. A. (2017). Prediction of heat-induced polymerization of different globular food proteins in mixtures with wheat gluten. *Food Chemistry*, *221*(8), 1158–1167. https://doi.org/10.1016/j.foodchem.2016.11.043

Lara, C., Gourdin-Bertin, S., Adamcik, J., Bolisetty, S., & Mezzenga, R. (2012). Self-assembly of ovalbumin into amyloid and non-amyloid fibrils. *Biomacromolecules*, *13*(12), 4213–4221. https://doi.org/10.1021/bm301481v

Leonil, J., Molle, D., Fauquant, J., Maubois, J. L., Pearce, R. J., & Bouhallab, S. (1997). Characterization by ionization mass spectrometry of lactosyl b-lactoglobulin conjugates formed during heat treatment of milk and whey and identification of one lactose-binding site. *Journal of Dairy Science*, *80*(10), 2270–2281. https://doi.org/10.3168/jds.2008-1263

Lobley, A., Whitmore, L., & Wallace, B. A. (2002). DICHROWEB: An interactive website for the analysis of protein secondary structure from circular dichroism spectra. *Bioinformatics*, *18*(1), 211–212. https://doi.org/10.1093/bioinformatics/18.1.211

Loveday, S., Anema, S., & Singh, H. (2017). β-Lactoglobulin nanofibrils: The long and the short of it. *International Dairy Journal*, *67*(4), 35–45. https://doi.org/10.1016/j.idairyj.2016.09.011

Loveday, S., Rao, M., Creamer, L., & Singh, H. (2009). Factors affecting rheological characteristics of fibril gels: The case of β-lactoglobulin and α-lactalbumin. *Journal of Food Science*, *74*(3), 47–55. https://doi.org/10.1111/j.1750-3841.2009.01098.x

Loveday, S., Su, J., Rao, M., Anema, S., & Singh, H. (2011). Effect of calcium on the morphology and functionality of whey protein nanofibrils. *Biomacromolecules*, *12*(10), 3780–3788. https://doi.org/10.1021/bm201013b

Loveday, S., Su, J., Rao, M., Anema, S., & Singh, H. (2012). Whey protein nanofibrils: The environment-morphology-functionality relationship in lyophilization, rehydration, and seeding. *Journal of Agricultural and Food Chemistry*, *60*(20), 5229–5236. https://doi.org/10.1021/jf300367k

Loveday, S., Wang, X., Rao, M., Anema, S., & Singh, H. (2012). β-Lactoglobulin nanofibrils: Effect of temperature on fibril formation kinetics, fibril morphology and the rheological properties of fibril dispersions. *Food Hydrocolloids*, *27*(1), 242–249. https://doi.org/10.1016/j.foodhyd.2011.07.001

Mackintosh, S., Meade, S., Healy, J., Sutton, K., Larsen, N., Squires, A., & Gerrard, J. (2009). Wheat glutenin proteins assemble into a nanostructure with unusual structural features. *Journal of Cereal Science*, *49*(1), 157–162. https://doi.org/10.1016/j.jcs.2008.08.003

Martin, A., Grolle, K., Bos, M., Cohen Stuart, M., & van Vliet, T. (2002). Network forming properties of various proteins adsorbed at the air/water interface in relation to foam stability. *Journal of Colloid and Interface Science*, *254*(1), 175–183. https://doi.org/10.1006/jcis.2002.8592

Meratan, A., Ghasemi, A., & Nemat-Gorgani, M. (2011). Membrane integrity and amyloid cytotoxicity: A model study involving mitochondria and lysozyme fibrillation products. *Journal of Molecular Biology*, *409*(5), 826–838. https://doi.org/10.1016/j.jmb.2011.04.045

Mezzenga, R., & Fischer, P. (2013). The self-assembly, aggregation and phase transitions of food protein systems in one, two and three dimensions. *Reports on Progress in Physics*, *76*(4), 046601. https://doi.org/10.1088/0034-4885/76/4/046601

Mills, C., Huang, L., Noel, T., Gunning, P., & Morris, V. (2001). Formation of thermally induced aggregates of the soya globulin β-conglycinin. *Biochimica et Biophysica Acta - Protein Structure and Molecular Enzymology*, *1547*(2), 339–350. https://doi.org/10.1016/S0167-4838(01)00199-6

Mine, Y. (2002). Recent advances in egg protein functionality in the food system. *World's Poultry Science Journal*, *58*(2), 31–39.

Mohammadian, M., & Madadlou, A. (2016). Cold-set hydrogels made of whey protein nanofibrils with different divalent cations. *International Journal of Biological Macromolecules*, *89*(8), 499–506. https://doi.org/10.1016/j.ijbiomac.2016.05.009

Mohammadian, M., Salami, M., Emam-Djomeh, Z., Momen, S., & Moosavi-Movahedi, A. (2018). Gelation of oil-in-water emulsions stabilized by heat-denatured and nanofibrillated whey proteins through ion bridging or citric acid-mediated cross-linking. *International Journal of Biological Macromolecules*, *120*(12), 2247–2258. https://doi.org/10.1016/j.ijbiomac.2018.08.085

Mohammadian, M., Salami, M., Momen, S., Alavi, F., Emam-Djomeh, Z., & Moosavi-Movahedi, A. (2019). Enhancing the aqueous solubility of curcumin at acidic condition through the complexation with whey protein nanofibrils. *Food Hydrocolloids*, *87*(8), 902–914. https://doi.org/10.1016/j.foodhyd.2018.09.001

Monge-Morera, M., Lambrecht, M., Deleu, L., Gallardo, R., Louros, N., De Vleeschouwer, M., … Delcour, J. A. (2020). Processing induced changes in food proteins : amyloid formation during boiling of hen egg white. *Biomacromolecules*, *21*(6), 2218–2228. https://doi.org/10.1021/acs.biomac.0c00186

Monge-Morera, M., Lambrecht, M., Deleu, L., Godefroidt, T., Goos, P., Rousseau, F., … Delcour, J. A. (2021). Drying mode and hydrothermal treatment conditions govern the formation of amyloid-like protein fibrils in solutions of dried hen egg white. *Food Hydrocolloids*, *112*(3), 106276. https://doi.org/10.1016/j.foodhyd.2020.106276

Monge-Morera, M., Lambrecht, M., Deleu, L., Louros, N., Rousseau, F., Schymkowitz, J., & Delcour, J. A. (2021). Heating wheat gluten promotes the formation of amyloid-like fibrils. *ACS Omega*, *6*(3), 1823–1833. https://doi.org/10.1021/acsomega.0c03670

Mudgal, P., Daubert, C., & Foegeding, E. (2009). Cold-set thickening mechanism of β-lactoglobulin at low pH: Concentration effects. *Food Hydrocolloids*, *23*(7), 1762–1770. https://doi.org/10.1016/j.foodhyd.2009.03.009

Munialo, C., Martin, A., van der Linden, E., & de Jongh, H. (2014). Fibril formation from pea protein and subsequent gel formation. *Journal of Agricultural and Food Chemistry*, *62*(11), 2418–2427. https://doi.org/10.1021/jf4055215

Murray, B. S. (2011). Rheological properties of protein films. *Current Opinion in Colloid and Interface Science*, *16*(1), 27–35. https://doi.org/10.1016/j.cocis.2010.06.005

Nelson, R., Sawaya, M., Balbirnie, M., Madsen, A., Riekel, C., Grothe, R., & Eisenberg, D. (2005). Structure of the cross-β spine of amyloid-like fibrils. *Nature*, *435*(6), 773–778. https://doi.org/10.1038/nature03680

Nicolai, T., & Durand, D. (2013). Controlled food protein aggregation for new functionality. *Current Opinion in Colloid and Interface Science*, *18*(4), 249–256.

https://doi.org/10.1016/j.cocis.2013.03.001

Nisbet, A., Saundry, R., Moir, A., Fothergill, L., & Fothergill, J. (1981). The complete amino-acid sequence of hen ovalbumin. *European Journal of Biochemistry*, *115*(2), 335–345. https://doi.org/10.1111/j.1432-1033.1981.tb05243.x

Oboroceanu, D., Wang, L., Kroes-Nijboer, A., Brodkorb, A., Venema, P., Magner, E., & Auty, M. (2011). The effect of high pressure microfluidization on the structure and length distribution of whey protein fibrils. *International Dairy Journal*, *21*(10), 823–830. https://doi.org/10.1016/j.idairyj.2011.03.015

Ow, S., & Dunstan, D. (2013). The effect of concentration, temperature and stirring on hen egg white lysozyme amyloid formation. *Soft Matter*, *9*(40), 9692–9701. https://doi.org/10.1039/b000000x

Pearce, G., Mackintosh, S., & Gerrard, J. (2007). Formation of amyloid-like fibrils by ovalbumin and related proteins under conditions relevant to food processing. *Journal of Agricultural and Food Chemistry*, *55*(2), 318–322. https://doi.org/10.1021/jf062154p

Poon, S., Clarke, A., & Schultz, C. (2001). Effect of denaturants on the emulsifying activity of proteins. *Journal of Agricultural and Food Chemistry*, *49*(1), 281–286. https://doi.org/10.1021/jf000179x

Rambaran, R. N., & Serpell, L. C. (2008). Amyloid fibrils: abnormal protein assembly. *Prion*, *2*(3), 112–117. https://doi.org/10.4161/pri.2.3.7488

Renkema, J., Lakemond, C., de Jongh, H., Gruppen, H., & van Vliet, T. (2000). The effect of pH on gel forming properties of soy proteins. *Journal of Biotechnology*, *79*(3), 223–230.

Rousseau, F., Serrano, L., & Schymkowitz, J. (2006). How evolutionary pressure against protein aggregation shaped chaperone specificity. *Journal of Molecular Biology*, *355*(5), 1037–1047. https://doi.org/10.1016/j.jmb.2005.11.035

Setiowati, A. (2018). *Emulsifying and stabilizing properties of whey protein- pectin conjugates prepared by dry heat treatment*. Ghent University.

Setiowati, A., De Neve, L., A'yun, Q., & Van der Meeren, P. (2021). Quartz Crystal Microbalance with Dissipation (QCM-D) as a tool to study the interaction between whey protein isolate and low methoxyl pectin. *Food Hydrocolloids*, *110*(1), 106180. https://doi.org/10.1016/j.foodhyd.2020.106180

Simpson, R. (2006). *Fragmentation of protein using trypsin. CSH protocols*. United States. https://doi.org/10.1101/pdb.prot4550

Sreerama, N., & Woody, R. W. (2000). Estimation of protein secondary structure from circular dichroism spectra : comparison of CONTIN , SELCON , and CDSSTR methods with an expanded reference set. *Analytical Biochemistry*, *287*(1), 252–260. https://doi.org/10.1006/abio.2000.4880

Stehfest, E., Bouwman, L., van Vuuren, D., den Elzen, M., Eickhout, B., & Kabat, P. (2009). Climate benefits of changing diet. *Climatic Change*, *95*(3), 83–102. https://doi.org/10.1007/s10584-008-9534-6

Stsiapura, V., Maskevich, A., Kuzmitsky, V., Uversky, V., Kuznetsova, I., & Turoverov, K. (2008). Thioflavin T as a molecular rotor: Fluorescent properties of thioflavin T in solvents with different viscosity. *Journal of Physical Chemistry B*, *112*(49), 15893–15902. https://doi.org/10.1021/jp805822c

Sulatskaya, A., Sulatsky, M., Antifeeva, I., Kuznetsova, I., & Turoverov, K. (2019). Structural analogue of thioflavin T, DMASEBT, as a tool for amyloid fibrils study. *Analytical Chemistry*, *91*(4), 3131–

3140. research-article. https://doi.org/10.1021/acs.analchem.8b05737

Sunde, M., Serpell, L., Bartlam, M., Fraser, P., Pepys, M., & Blake, C. (1997). Common core structure of amyloid fibrils by synchrotron X-ray diffraction. *Journal of Molecular Biology*, *273*(3), 729–739. https://doi.org/10.1006/jmbi.1997.1348

Swaminathan, B., Ravi, V., Kumar, S., Venkata, M., Kumar, S., & Chandra, N. (2011). Lysozyme: a model protein for amyloid research. *Advances in Protein Chemistry and Structural Biology*, *84*(1), 63–111. https://doi.org/10.1016/B978-0-12-386483-3.00003-3

Tanaka, N., Morimoto, Y., Noguchi, Y., Tada, T., Waku, T., Kunugi, S., … Takahashi, N. (2011). The mechanism of fibril formation of a non-inhibitory serpin ovalbumin revealed by the identification of amyloidogenic core regions. *Journal of Biological Chemistry*, *286*(7), 5884–5894. https://doi.org/10.1074/jbc.M110.176396

Tcholakova, S., Denkov, N., Ivanov, I., & Campbell, B. (2002). Coalescence in b-lactoglobulin-stabilized emulsions : effects of protein adsorption and drop size. *Langmuir*, *18*(23), 8960–8971.

Tcholakova, S., Denkov, N., Sidzhakova, D., Ivanov, I., & Campbell, B. (2003). Interrelation between drop size and protein adsorption at various emulsification conditions. *Langmuir*, *19*(13), 5640–5649.

van der Linden, E., & Venema, P. (2007). Self-assembly and aggregation of proteins. *Current Opinion in Colloid and Interface Science*, *12*(10), 158–165. https://doi.org/10.1016/j.cocis.2007.07.010

Van Kleef, F. (1986). Thermally induced protein gelation: gelation and rheological characterization of highly concentrated ovalbumin and soybean protein gels. *Biopolymers*, *25*(1), 31–59. https://doi.org/10.1002/bip.360250105

Wang, S., Chen, P., & Hung, Y. (2006). Effects of p -benzoquinone and melatonin on amyloid fibrillogenesis of hen egg-white lysozyme. *Journal of Molecular Catalysis B: Enzymatic*, *43*(1), 49–57. https://doi.org/10.1016/j.molcatb.2006.06.006

Wei, Z., Cheng, J., & Huang, Q. (2019). Food-grade Pickering emulsions stabilized by ovotransferrin fibrils. *Food Hydrocolloids*, *94*(3), 592–602. https://doi.org/10.1016/j.foodhyd.2019.04.005

Weijers, M., Sagis, L., Veerman, C., Sperber, B., & van der Linden, E. (2002). Rheology and structure of ovalbumin gels at low pH and low ionic strength. *Food Hydrocolloids*, *16*(3), 269–276. https://doi.org/10.1016/S0268-005X(01)00097-2

Whitmore, L., & Wallace, B. A. (2004). DICHROWEB, an online server for protein secondary structure analyses from circular dichroism spectroscopic data. *Nucleic Acids Research*, *32*(13), 668–673. https://doi.org/10.1093/nar/gkh371

WHO. (2007). Protein and amino acid requirement in nutrition. *World Health Organization Technical Report Series*, *935*(1), 1–265.

Xue, C., Lin, T. Y., Chang, D., & Guo, Z. (2017). Thioflavin T as an amyloid dye: Fibril quantification, optimal concentration and effect on aggregation. *Royal Society Open Science*, *4*(1). https://doi.org/10.1098/rsos.160696

Zayas, J. (1997). *Functionality of proteins in food*. Springer Berlin Heidelberg. https://doi.org/10.1007/978-3-642-59116-7

Zhang, Y., & Huang, L. (2014). Effect of heat-induced formation of rice bran protein fibrils on morphological structure and physicochemical properties in solutions and gels. *Food Science and Biotechnology*, *23*(5), 1417–1423. https://doi.org/10.1007/s10068-014-0194-1

Zhao, D., Li, L., Xu, D., Sheng, B., Qin, D., Chen, J., … Zhang, X. (2018). Application of ultrasound pretreatment and glycation in regulating the heat-induced amyloid-like aggregation of β-lactoglobulin. *Food Hydrocolloids*, *80*(7), 122–129. https://doi.org/10.1016/j.foodhyd.2018.02.001